Flood risk assessment for Indian sub-continental river basins

Urmin Vegad[1], Yadu Pokhrel[2], and Vimal Mishra[1,3*]

[1]Civil Engineering, Indian Institute of Technology (IIT) Gandhinagar

[2]Department of Civil and Environmental Engineering, Michigan State University, East Lansing, Michigan, USA

[3]Earth Sciences, Indian Institute of Technology (IIT) Gandhinagar

*Corresponding author: vmishra@iitgn.ac.in

Abstract

Floods are among India's most frequently occurring natural disasters, which disrupt all aspects of socio-economic well-being. A large population is affected by floods during almost every summer monsoon season in India, leaving its footprint through human mortality, migration, and damage to agriculture and infrastructure. Despite the massive imprints of floods, sub-basin level flood risk assessment is still in its infancy and requires advancements. Using hydrological and hydrodynamical models, we reconstructed sub-basin level observed floods for the 1901-2020 period. Our modelling framework includes the influence of 51 major reservoirs that affect flow variability and flood inundation. Sub-basins in the Ganga and Brahmaputra River basins witnessed substantial flood inundation extent during the worst flood in the observational record. Major floods in the sub-basins of the Ganga and Brahmaputra occur during the late summer monsoon season (August-September). Beas, Brahmani, upper Satluj, Upper Godavari, Middle and Lower Krishna, and Vashishti sub-basins are among the most influenced by the dams, while Beas, Brahmani, Ravi, and Lower Satluj are among the most impacted by floods and the presence of dams. Bhagirathi, Gandak, Kosi, lower Brahmaputra, and Ghaghara are India's sub-basins with the highest flood risk. Our findings have implications for flood risk assessment and mitigation in India.

1. Introduction

Flood risk to both natural and human systems is projected to increase due to climate change (IPCC, 2014, 2022). Extreme weather and climate extremes have increased under warming climate, leading to an increased frequency of natural hazards like floods, droughts, heat waves, cyclones, and heavy rains. Hydroclimatic extremes affect humans and infrastructure (Eidsvig et al., 2017; Peduzzi et al., 2009). Due to high vulnerability and lower adaptive capacity, developing countries are often the most impacted by extreme weather events. Further, developing countries usually take longer to recover from the hazards due to low climate resilience. Globally, floods are among the most devastating natural hazards (Ghosh & Kar, 2018). Among all flood types, riverine floods occur most frequently (Kimuli et al., 2021) and often cause substantial damage to agriculture and infrastructure. A considerable fraction of the population and infrastructure are exposed to flooding, which will also increase due to the projected increase in the magnitude and frequency of floods (Winsemius et al., 2018).

The increase in flood magnitude due to the warming climate has resulted in considerable economic losses (C. M. R. Mateo et al., 2014; Willner et al., 2018). The total financial loss will likely increase by 17% in the next 20 years due to climate change (Willner et al., 2018). Besides agriculture, floods significantly affect the built environment and transportation infrastructure (Kalantari et al., 2014). For instance, more than 7% of road and railway assets

globally are exposed to a 100-year return period flood (Koks et al., 2019). In Asia, about 75% of the population is exposed to riverine floods (Varis et al., 2022). India falls among the top ten most flood-affected countries in Asia and the Pacific (Kimuli et al., 2021). In addition, India is also among the top-ten countries that experienced the highest human mortality due to floods. Considerable population exposure, climate change, and rapid growth and development in flood-prone areas contribute to increased losses from floods.

In India, state administration takes decisions to mitigate floods while the central government provides financial aid under severe conditions (Jain et al., 2017). The state authorities develop action plans to minimize flood damage. Therefore, identifying the regions with higher flood risk is essential for planning and mitigation. Flood impacts can be quantified according to the affected population, gross domestic product (GDP), and agricultural practices (Ward et al., 2013). The flood risk assessment framework suggested by the Intergovernmental Panel on Climate Change (IPCC) has been extensively applied at the regional and global scales (Allen et al., 2016; IPCC, 2014; Roy et al., 2021). The risk can be quantified as a function of vulnerability, hazard, and exposure (IPCC, 2014). To control the risk, reducing vulnerability is considered a short to the mid-term goal (V. Mishra et al., 2022), while reducing hazards and exposure are long-term goals (Birkmann & Welle, 2015). Flood risk assessment can assist in identifying the regions at high risk due to higher vulnerability, hazard, and exposure, which can be used for developing a framework, methodology, and guidelines for flood mitigation and damage assessment.

A flood risk assessment performed on a global scale may not help in identifying the flood risk-prone regions at a country scale due to the coarser spatial resolution (Bernhofen et al., 2022). Due to complex geomorphological characteristics and diverse climatic conditions, India is considered a relatively high flood-risk region (Hochrainer-Stigler et al., 2021). Therefore, estimating flood risk on a finer scale (e.g. sub-basin level) is essential for reliable flood risk assessment. There have been studies on regional or river basin scales (Allen et al., 2016; Ghosh & Kar, 2018; Roy et al., 2021); however, those do not provide flood risk at a sub-basin scale in India. In addition, the impact assessment of floods on transport infrastructure (rail and road infrastructure) still needs to be improved in the country (Pathak et al., 2020; P. Singh et al., 2018). In addition, the role of dams and reservoirs in the flood risk assessment should be addressed (Hirabayashi et al., 2013; Yamazaki et al., 2018a). Dams and reservoirs considerably influence streamflow variability and can attenuate flood peaks (Dang et al., 2019; Vu et al., 2022; Zajac et al., 2017). In contrast, dam operations and decisions can also worsen the flood situation in the downstream regions. For instance, recent flooding in Kerala and Chennai was partly attributed to reservoir operations (V. Mishra & Shah, 2018). India has more than 5300 large dams regulating river flow (National Register of Large Dams (NRLD), 2019), affecting ecosystems, natural resources, and livelihoods (Acreman, 2000). Reservoirs impact flow regulation, magnitude, timing, and extent of flooding in the downstream regions. Therefore, flood risk assessment without considering the role of reservoirs can be inappropriate in the basins that are highly affected by the presence of dams.

We use the H08 (Hanasaki et al., 2018) global hydrological model combined with the CaMa-Flood (Yamazaki et al., 2011) model for the sub-basin level flood risk assessment in India considering the role of reservoirs. The CaMa-Flood model combined with the H08 model has been used for several river basins globally (Boulange et al., 2021; C. M. R. Mateo et al., 2013). The CaMa-Flood model performs well in simulating flood dynamics (Chaudhari and Pokhrel, 2022; H. Dang et al., 2022; Gaur & Gaur, 2018; Hirabayashi et al., 2013, 2021; Yamazaki et al., 2018; Yang et al., 2019). The CaMa-Flood model takes runoff as input simulated from any hydrological

model and can simulate flood depth and inundation. In India, almost all the major rivers are influenced by reservoirs (Lehner et al., 2011). Therefore, the major scientific questions that we address are: 1) How does the flood risk vary at the sub-basin level in India during the 1901-2020 period? 2) Which are the sub-basins where the presence of reservoirs considerably influences the flood risk? To address these questions, we use long-term observations (1901-2020) from India Meteorological Department (IMD) along with a hydrological modelling framework.

2. Data and Methods

2.1 Datasets

We used observed gridded precipitation (Pai et al., 2014) and daily maximum and minimum temperatures (Srivastava et al., 2009) from India Meteorological Department (IMD). We obtained gridded daily precipitation at 0.25° from IMD for the 1901-2020 period that was developed using station-based rainfall observations from more than 6900 gauge stations (Pai et al., 2014). The gridded rainfall product has been widely used for hydrological studies (Kushwaha et al., 2021; Shah & Mishra, 2016) and it captures the key features of the summer monsoon variability and orographic rainfall over the western Ghats and foothills of the Himalayas. We obtained daily 1° gridded maximum and minimum temperatures from IMD (Srivastava et al., 2009). The gridded temperature dataset is developed using observations from 395 stations located across India. Bilinear interpolation was used to convert the 1° gridded temperature to 0.25° resolution to make it consistent with the gridded precipitation. For the regions outside India, we obtained observational meteorological datasets (rainfall and temperature) at 0.25 degrees from Princeton University (Sheffield et al., 2006). Gridded datasets from Sheffield et al. (2006) compare well against the IMD observations and have been used in hydrological applications in India (Shah & Mishra, 2016).

Observed daily streamflow at gauge stations and reservoir live storage were obtained from India Water Resources Information System (India-WRIS). We considered the influence of 51 major reservoirs located in different river basins to examine the impact of reservoirs on floods using the CaMa-Flood model (Figure S1). The information of dams was obtained from the National Register of Large Dams (NRLD) [Table S1]. We used the Global Surface Water (GSW) extent to estimate flood occurrences at a monthly timescale (Pekel et al., 2016). Simulated flood occurrences during the period of the GSW database (1985-2020) were used to validate the performance of the hydrological model in simulating flood extent (Pekel et al., 2016). In addition, we obtained reported flood details from the Emergency Events Database (EM-DAT, http://www.emdat.be/) and Dartmouth Flood Observatory (DFO, http://floodobservatory.colorado.edu/). EM-DAT is developed by the Centre for Research on the Epidemiology of Disasters (CRED), while the University of Colorado manages DFO. We used population data from Global Human Settlement Layers (GHLS) to estimate flood exposure. Finally, we used roadway and railway network data to assess the impact of floods on the infrastructure.

2.2 H08-CaMa-Flood combined model

We used the H08 (Hanasaki et al., 2018) global hydrological model to simulate hydrological variables. The H08 is a distributed global water resources model comprising six sub-models: land surface hydrology, river routing, reservoir operation, crop growth, environmental flow, and water abstraction. The model estimates baseflow using a leaky bucket method, while runoff is calculated based on saturation excess non-linear flow (Hanasaki et al.,

2008). The H08 model can be run separately or combined with any hydrodynamic model to perform flow routing. The H08 model uses precipitation, air temperature, short and longwave radiations, wind speed, surface pressure, and specific humidity as input meteorological forcing. Soil parameters for the H08 model were obtained from Harmonized World Soil Database (HWSD). We forced the H08 model with the input meteorological forcing at 0.25° spatial and daily temporal resolution. We combined the H08 land surface model with the CaMa-Flood model. The CaMa-Flood model has been previously combined with the H08 model to obtain flood inundation estimates (C. M. Mateo et al., 2014).

The CaMa-Flood (version 4.1) is a hydrodynamic model (Yamazaki et al., 2011), which simulates river-floodplain dynamics (Yamazaki et al., 2013). The CaMa-Flood model has been extensively used for better performance in simulating discharge and flood peaks (Zhao et al., 2017). The CaMa-Flood model considers the role of dams and reservoirs for streamflow and flood inundation simulations (Chaudhari & Pokhrel, 2022; C. M. Mateo et al., 2014; Pokhrel et al., 2018). We ran the CaMa-Flood model at a finer spatial resolution (0.1°) using the H08-simulated runoff (0.25°) as input. We calibrated the combined model (H08 and CaMa-Flood) for India's eighteen major river basins for at least one gauge station each, considering the influence of 51 major dams. The gauge stations were selected in the farthest downstream of the river basin based on the availability of observed streamflow. The influence of reservoir operations was simulated using the CaMa-Flood model and evaluated against the observed daily live reservoir storage.

Large-scale global hydrological models do not perfectly capture the observed trends and variations as these are often not well calibrated at river basin scale (Krysanova et al., 2018). The H08 model performs well when calibrated at the river basin scale rather than coarser domains such as climate zones (Chuphal & Mishra, 2023; Yoshida et al., 2022). Here, we manually calibrated the H08 model by adjusting four key parameters that considerably influence streamflow for each river basin, which include single-layer soil depth, gamma, bulk transfer coefficient, and tau (Hanasaki et al., 2008; Raghav & Eldho, 2023). A more detailed discussion about the calibration parameters of H08 are discussed in Dangar & Mishra (2021). Different sets of combinations of calibration parameters within a range were used to calibrate the H08 model. The employed sets of parameters for the 18 river basins in the Indian sub-continent are listed in Table S2. The calibrated parameters account for the effect of human interventions because the model calibration is performed against the observed streamflow rather than the naturalized streamflow (Duc Dang et al., 2020). We evaluated the model performance using the coefficient of determination (R^2) and Nash-Sutcliffe Efficiency (NSE) for daily streamflow and reservoir live storage. In addition, we compared the simulated and satellite-based observed flood occurrences. The satellite-based flood occurrence is calculated using the Global Surface Water (GSW) dataset (Pekel et al., 2016), available for the 1984-2020 period. We forced the well-calibrated combined (H08 and CaMa-Flood) models with observed meteorological forcing from India Meteorological Department (IMD) at 0.25° spatial resolution to conduct simulations from 1901 to 2020. The H08 model simulated runoff is used in CaMa-Flood to rout flood dynamics at six arc-minutes (0.1 degrees). We generated the flood depth maps for the historical worst flood at the sub-basin level. The worst flood is based on the highest magnitude of river flow observed at the subbasin outlet. The generated flood depths at 6 arc-minutes (0.1°) were further downscaled to 1 arc-minute (~0.185 km) resolution using the downscaling module available within the CaMa-Flood.

We used C-ratio (Nilsson et al., 2005; Zajac et al., 2017) to assess the potential impact of dams along a river. The C-ratio is an identifier calculated as the ratio of total maximum storage capacity of the upstream reservoirs to the mean annual discharge at a gauge station in the downstream region (Nilsson et al., 2005; Zajac et al., 2017). We calculated the C-ratio at the outlets of each sub-basins that are influenced by the presence of dams. A C-ratio of less than 0.5 indicates that the sub-basin is minimally affected by the presence of dams. Further, to identify sub-basins susceptible to flood inundation resulting from dam operations, we multiplied the percentage of flooded area in each sub-basin by its corresponding C-ratio. This enabled us to identify the sub-basins that experience substantial flood inundation and are considerably impacted by the presence of reservoirs. Finally, we estimated the exposed rail and road infrastructure affected by floods. The flooded area overlapped over the road and railway network to estimate the network length affected by floods in a sub-basin. We considered the flooded area of the observed worst flood. The subbasins with the highest rail and road infrastructure exposure to floods were identified.

2.3 Risk assessment

We estimated flood risk using hazard, exposure, and vulnerability based on the common framework adopted by the United Nations in the Global Assessment Reports of the United Nations Office for Disaster Risk Reduction (UNISDR, 2011, 2013). A similar framework was used in previous studies for flood risk assessments (C. M. R. Mateo et al., 2014; Tanoue, 2020; Winsemius et al., 2013). We multiplied the normalized values of hazard, exposure, and vulnerability to estimate the risk as:

$$Risk = Vulnerability * Exposure * Hazard \quad \ldots\ldots (1)$$

The flood risk assessment can help identify the hotspots and prioritize climate adaptation (de Moel et al., 2015). Among the three components, vulnerability is a degree of damage to a particular object at flood risk with a specified amount and present on a scale from 0 to 1. We obtained the vulnerability index for each district from the "Climate Vulnerability Assessment for Adaptation Planning in India Using a Common Framework", a report developed by the Department of Science and Technology (https://dst.gov.in/sites/default/files/Full%20Report%20%281%29.pdf). The vulnerability of each district is calculated using 14 indicators, each with equal weights. The indicators capture both sensitivity and adaptive capacity. We estimated the vulnerability index of each sub-basin by taking the spatial mean of the vulnerability of the districts falling into the sub-basins. Exposure is termed as assets and population in a flood-exposed area resulting in flood damage (Marchand et al., 2022). The population dataset is a critical component in performing exposure estimation. The exposure is defined as the fraction of the population exposed to the flood extent (Smith et al., 2019). We completed the flood exposure estimate using the Global Human Settlement Layers (GHSL) population dataset (Joint Research Centre (JRC) et al., 2021), which is available at a resolution of 30 arc-seconds for 1975, 1990, 2000, 2014 and 2015. We used the population data for the year 2015 throughout this study. We rescaled the population data to 6 arc-minutes to make it consistent with the flooded area simulated from the combined model. We estimated the hazard as the exceedance probability of a flooded area exceeding half of the historical maximum flooded area in the last 50 years. We used normalized vulnerability, exposure, and hazard to estimate the risk.

3. Results

3.1 Calibration and evaluation of hydrological models

We calibrated and evaluated the performance of the H08 and CaMa-Flood combined models against the observed daily streamflow (Figure 1). Due to the unavailability of daily observed streamflow for the three transboundary river basins (Indus, Ganga and Brahmaputra), we used observed monthly streamflow to calibrate the model. In addition, we evaluated the model performance for daily live storage of the 51 reservoirs after the calibration against the observed flow (Figure 1). The model exhibited good skills ($R^2 > 0.6$ and NSE > 0.6) for almost all the river basins except Cauvery, East Coast, Northeast Coast, and Sabarmati. The model also performed well with NSE greater than 0.6 for more than 80% of the selected reservoirs in simulating daily live storage for the selected reservoirs. We estimated the bias and timing error in simulating peak discharge at all the selected gauge stations (Figure S2). We calculated the bias in the model simulated annual maximum streamflow against the observed annual maximum streamflow for the time periods for which observations are available. We excluded the transboundary rivers (Ganga, Brahmaputra and Indus) as timing error (in days) could not be estimated due to the unavailability of daily observed flow. While other gauge stations exhibited moderate bias, gauge stations in Cauvery, Sabarmati, and Mahi rivers basins show a considerable dry bias. Contrary to several other stations where the mean timing error was below two days, the Sabarmati river basin displayed a comparatively higher mean timing error. The relatively poor performance of the model in these river basins can be attributed to the lack of long-term observations as well as substantial human interventions that can affect the observed flow.

We compared model-simulated, and satellite-based observed flood occurrence for the 1984-2020 period (Figure 2). In addition, we compared the model-simulated flood events against Sentinel-1 SAR and MODIS satellite-based imagery for a few flood events based on the satellite data availability (Figures. 3, S3, S4). We found that the model simulated flood extent captures the satellite based flood extent. However, we note that the model overestimated the flood extent in Ganga river basin and underestimated in Brahmaputra river basin, therefore, showing a non-systematic bias. Moreover, a considerable difference in the flood extent based on the two satellite datasets was observed, which highlights the observational uncertainty in the estimation of flood extent. In general, the model exhibits satisfactory performance in simulating flood extent against the satellite-based observations. However, the model overestimates flood extent in the Ganga basin, which could be attributed to the influence of cloud contamination and dense vegetation cover on satellite-based flood estimates (Chaudhari & Pokhrel, 2022). On the other hand, the model underestimates the flood occurrence in the upstream region of the Brahmaputra River. This could be due to limitations in model parameterization, as observed flow is limited in the transboundary river basins. Despite the good performance against the observed streamflow, the simulated flood extent has a considerable bias, which can be attributed to satellite-based flood extent mapping limitations and the model's ability to capture the flood extent accurately. The model-simulated flood extent shows a good agreement against the reported flood from EM-DAT and DFO databases (Figure S5). In addition, the simulated flood extent also showed a good agreement with the reported flood in cities in the Brahmaputra and Ganga River basins. Given the limitation in the streamflow and flood extent observations, the hydrological models perform satisfactorily and can be used for the sub-basin level risk assessment.

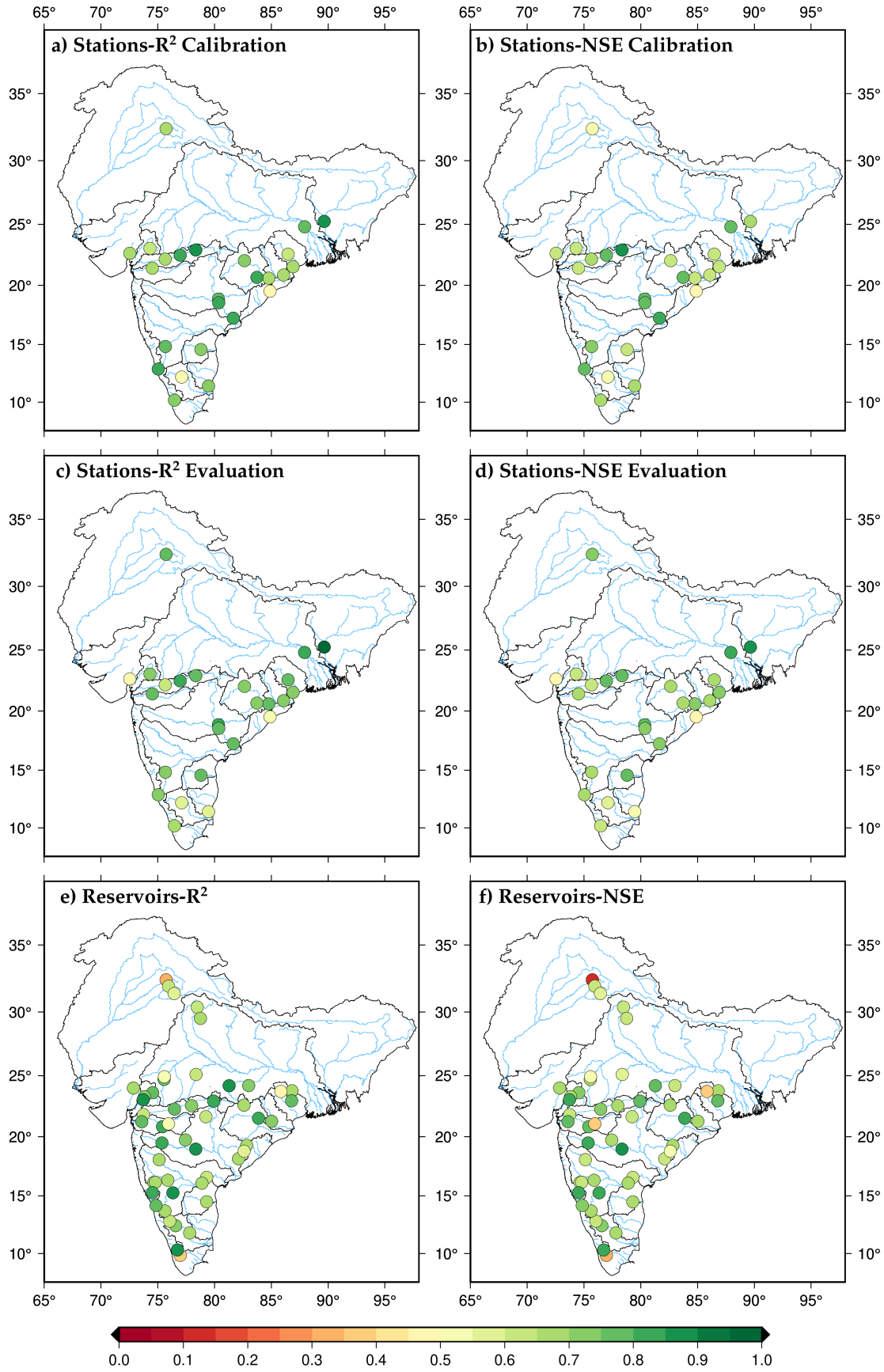

Figure 1: Calibration and evaluation of the combined model for daily river flow and reservoir storage at gauge stations and daily live storage of reservoirs

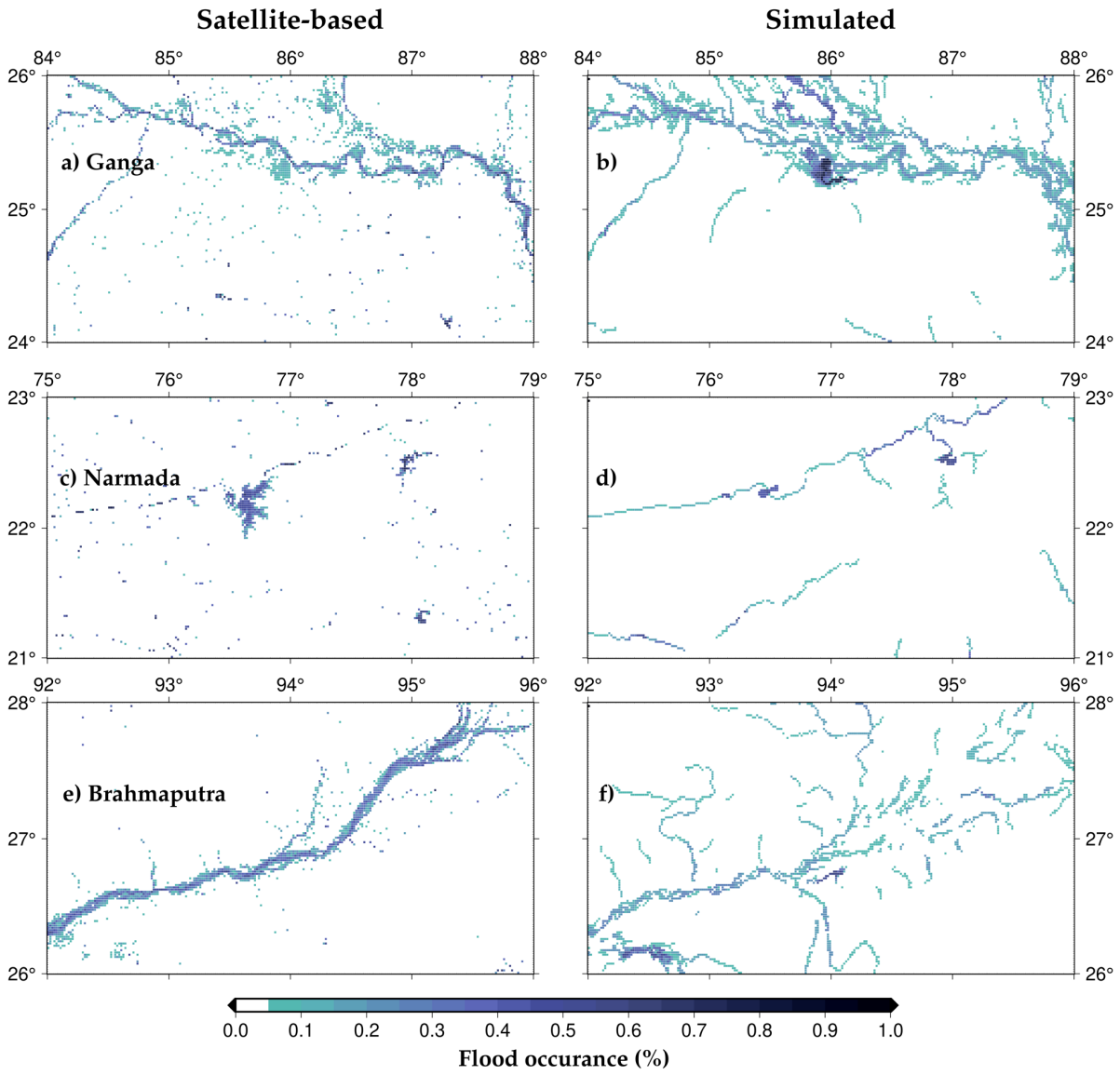

Figure 2: Simulated flood occurrences compared with satellite-based flood occurrence for different regions in Ganga, Narmada and Brahmaputra River basin.

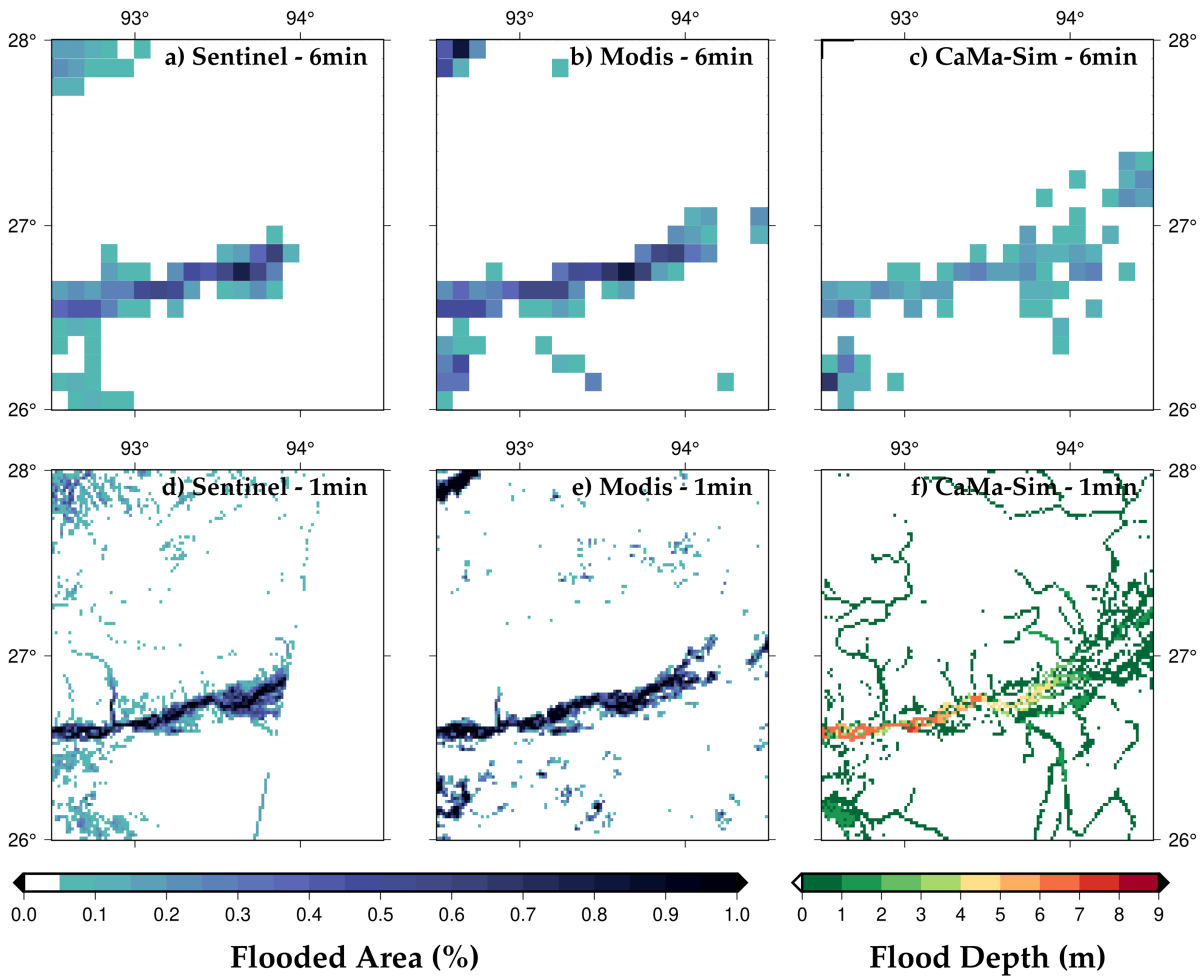

Figure 3: Simulated flood extent compared with Sentinel-1 SAR and MODIS satellite-based flood extent for the 2016 flood event in the Brahmaputra river

3.2 Estimation of the observed flood extent

Next, we reconstructed the flood inundation for the observed worst flood for each sub-basin for the 1901-2020 period in India. The inundation extent for the worst flood can help us identify the sub-basin with higher flood risk. We estimated flood depth and inundated area for each sub-basin for the worst flood during the last 120 years (Figure 4). In addition, we identified the occurrence of the worst flood at the sub-basin level during the 1901-2020 period. We highlighted ten sub-basins that experienced the highest fractional area affected by the worst flood. Sub-basins in the Ganga and Brahmaputra rivers are among the most highly influenced by the worst flood. For instance, Ghaghra, Kosi, Bhagirathi, Gandak, Gomti, lower Sabarmati, upper Yamuna, Ramganga, and Baitarani sub-basins had the highest fractional area affected by the worst flood during 1901-2020 (Figure 4). The fractional area of sub-basins in the semi-arid western India is less affected compared to those located in the Ganga basin. For example, the lower Sabarmati sub-basin of the Sabarmati River basin is among the sub-basins that are highly influenced by the observed worst flood. We also find that the worst flood in the same year did not affect all the sub-basins within a river basin (Figure S6). For instance, all the highly influenced sub-basins experienced the worst flood in different years in the Ganga basin (Figure 4). Most of the top flood-affected sub-basins experienced floods during August-September in the summer monsoon season. Overall, the flood extent due to the worst flood

250 is substantially greater in the sub-basins of the Ganga and Brahmaputra river basins compared to other basins in
251 India (Figure 4). Ganga river basin also has the highest population density among all the basins in the Indian sub-
252 continent, which makes it vulnerable for the flood risk.

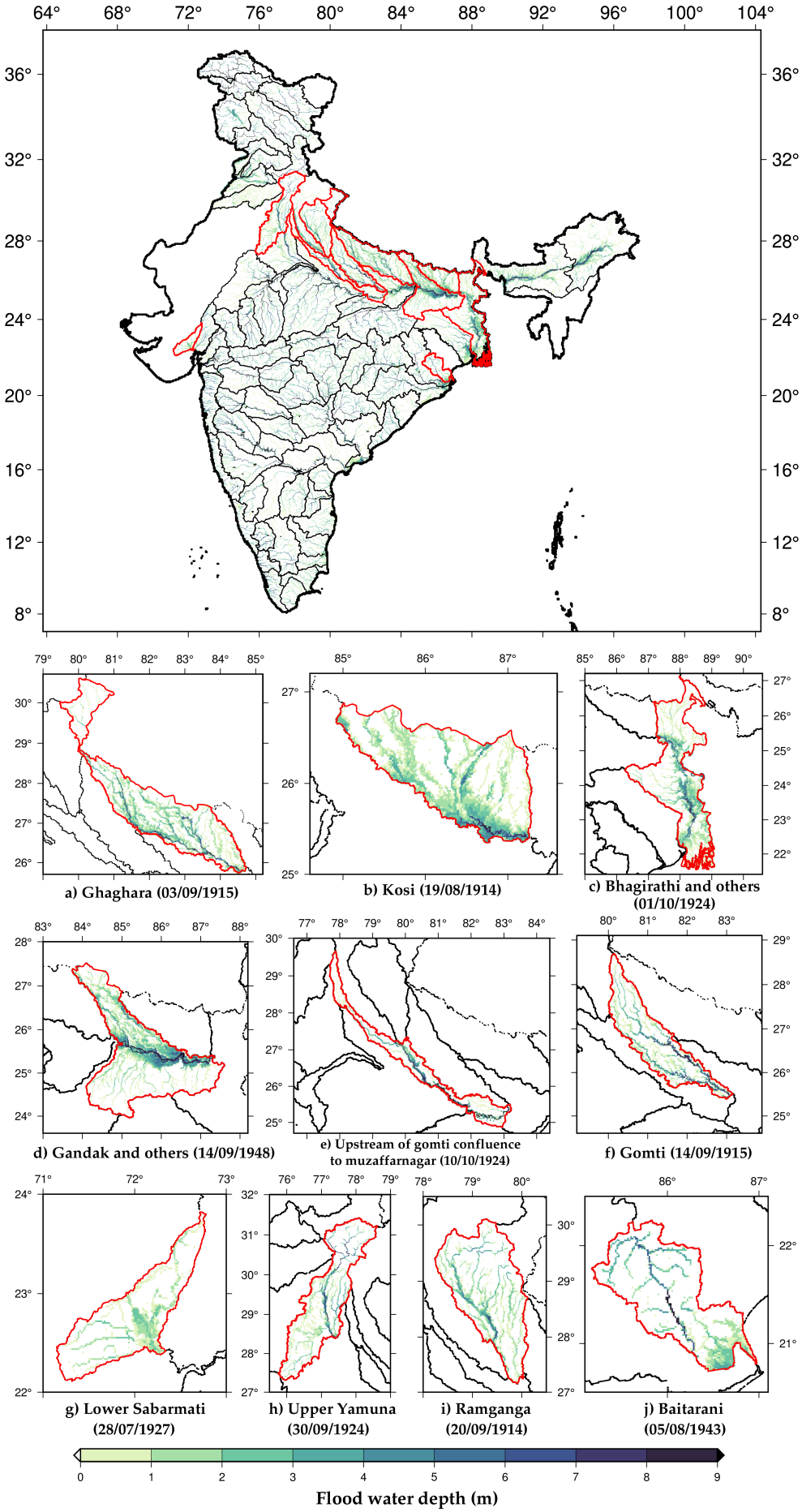
a) Ghaghara (03/09/1915)
b) Kosi (19/08/1914)
c) Bhagirathi and others (01/10/1924)
d) Gandak and others (14/09/1948)
e) Upstream of gomti confluence to muzaffarnagar (10/10/1924)
f) Gomti (14/09/1915)
g) Lower Sabarmati (28/07/1927)
h) Upper Yamuna (30/09/1924)
i) Ramganga (20/09/1914)
j) Baitarani (05/08/1943)
0 1 2 3 4 5 6 7 8 9
Flood water depth (m)

253

Figure 4: Flood depth map for the observed worst flood for each sub-basins, highlighting the sub-basins with maximum flood inundated area (%) (a) Ghaghara – Ganga River basin (b) Kosi – Ganga River basin (c) Bhagirathi and others – Ganga River basin (d) Gandak and others – Ganga River basin (e) Upstream of Gomti confluence to Muzaffarnagar – Ganga River basin (f) Gomti – Ganga River basin (g) Lower Sabarmati – Sabarmati River basin (h) Upper Yamuna – Ganga River basin (i) Ramganga – Ganga River basin (j) Baitarani – Brahmani River basin

Next, we examined the precipitation, streamflow, and flood-affected area (%) for the ten sub-basins that had the highest fractional flood affected area for the worst flood during 1901-2020 (Figure 5). As floods mostly occur during the summer monsoon season in India (V. Mishra et al., 2022; Nanditha & Mishra, 2021), we examined the temporal variability of precipitation, and streamflow during the monsoon season of the worst flood year. Nanditha and Mishra (2022) reported that multi-day precipitation is India's most robust driver of floods. Moreover, extreme precipitation and wet-antecedent conditions trigger floods in India (Nanditha & Mishra, 2022). We find that the Ghaghara sub-basin of the Ganga river experienced the worst flood in September 1915, affecting more than 10,000 km^2 area of the sub-basin. A multi-day rainfall in late August and early September (1915) caused the worst flood in the basin. The Kosi sub-basin of the Ganga river experienced the worst flood in August 1914, which affected more than 5000 km^2 of the basin (Figure 5). Similarly, Bhagirathi and other sub-basins in the Ganga river basin were affected by the worst flood in late September 1924, which inundated more than 12000 km^2 of the sub-basin. Similarly, Gandak and Gomti river basins experienced the worst floods in 1948 and 1915, respectively. Our results agree with the information presented in previous studies (Agarwal & Narain, 1991; Fredrick, 2017; Joshi, 2014; D. K. Mishra, 2015; A. Singh et al., 2021). We find that most of the sub-basins of the Ganga river basin are prone to large extents of flood inundation. Moreover, the worst floods in most sub-basins were caused by multi-day precipitation, a prominent driver of floods in the Indian sub-continental river basins (Figure 5).

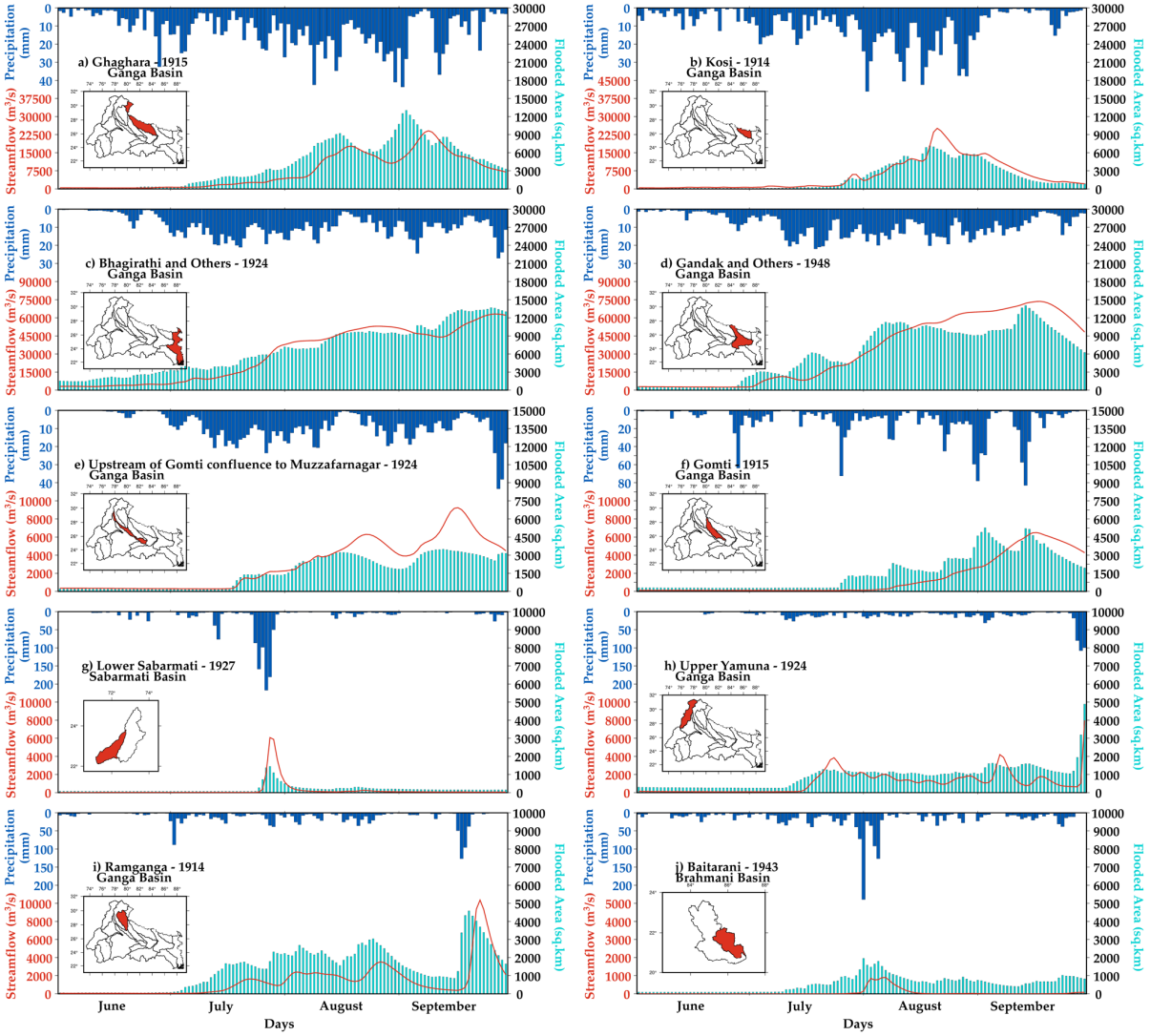

Figure 5: Daily upstream precipitation (mm, blue), the H08 model simulated streamflow (red) at the sub-basin outlet (m3/s), and flooded area (km2, green) for the summer monsoon (June-September) period of the corresponding worst flood year. (a) Ghaghara - Ganga River basin (b) Kosi - Ganga River basin (c) Bhagirathi and others - Ganga River basin (d) Gandak and others - Ganga River basin (e) Upstream of Gomti confluence to Muzaffarnagar - Ganga River basin (f) Gomti - Ganga River basin (g) Lower Sabarmati – Sabarmati River basin (h) Upper Yamuna – Ganga River basin (i) Ramganga – Ganga River basin (j) Baitarani – Brahmani River basin

To further examine the flood-affected area at the sub-basin level, we estimated the mean annual maximum flooded area (Figure 6a) and historical maximum flooded area using the H08-CaMa flood models (Figure 6b). Most of the highly flooded sub-basins are in the Ganga River basin. While the mean annual maximum flooded area for the top flood-affected sub-basins ranged between 10 to 15%, their maximum flooded area varied between 30 to 40%. Other than sub-basins from the Ganga river basin, Baitarani, lower Tapi, lower Godavari, Brahmani, and lower Mahanadi also showed a considerable mean flooded area during the 1901-1920 period. In the case of the maximum flooded area, Gandak, Kosi, and Ghaghara confluence to Gomti confluence sub-basins exhibited more than 20% flooded area. Sub-basins from the other river basins, such as lower Tapi, lower Narmada, Baitarani, and lower

Satluj, are in the top fifteen sub-basins with the highest flooded area. The sub-basins in the Ganga and Brahmaputra rivers are the most flood-affected. Moreover, the Ganga and Brahmaputra rivers experience the highest floods among all the river basins (Mohanty et al., 2020; Mohapatra & Singh, 2003).

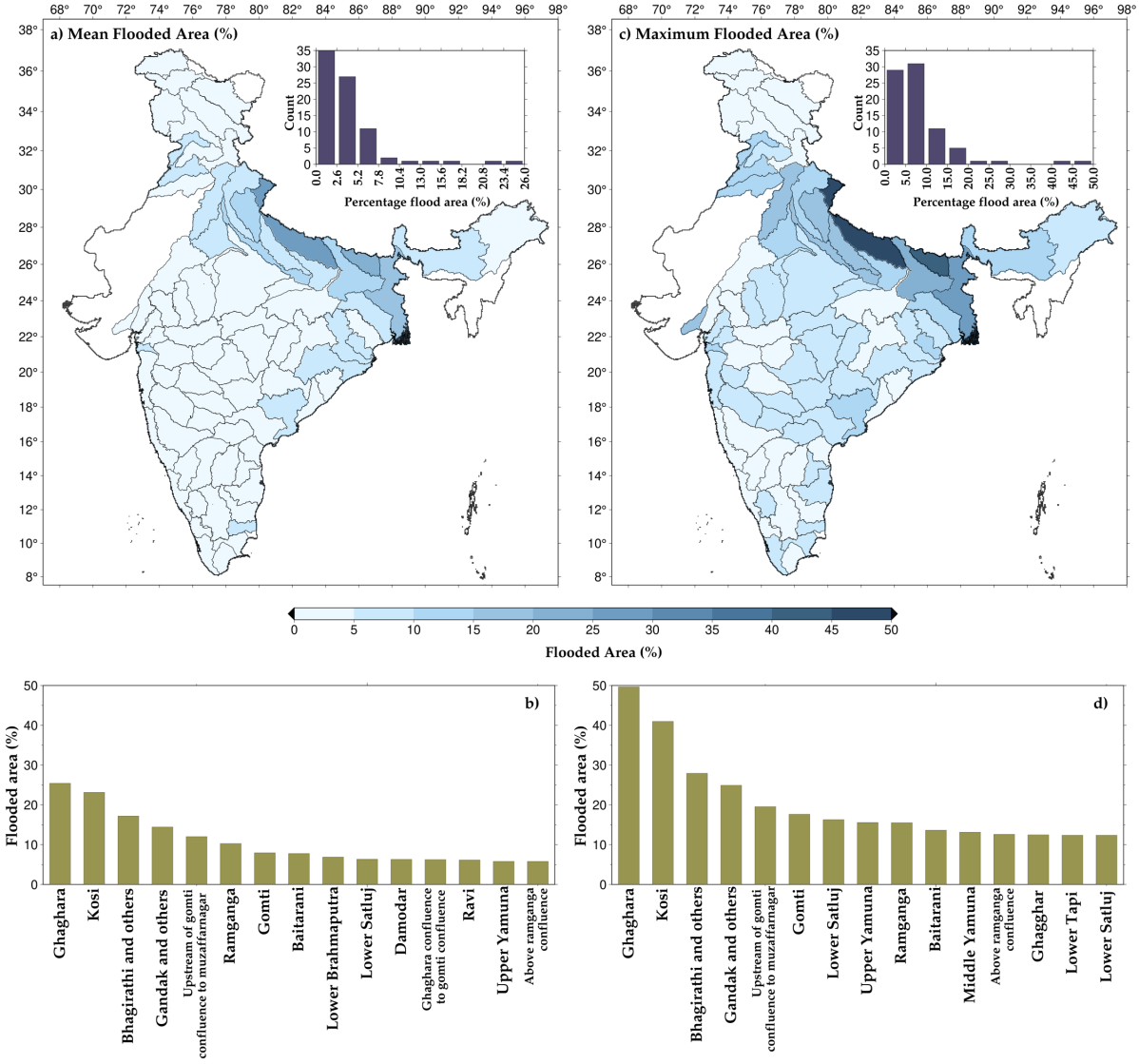

Figure 6: (a) Mean of annual maximum flooded area (percentage) between 1901-2020 and the overall distribution (b) highlighting the top fifteen sub-basin. (c) Historical maximum flooded area (percentage) and the overall distribution (d) highlighting the top fifteen sub-basin.

3.3 Influence of reservoirs on flood extent

We selected and considered 51 major reservoirs to examine their influence on flood risk based on the availability of the observed storage data. We estimated C-ratio for each sub-basin considering the river flow at the outlet to investigate the impact of reservoirs on streamflow. C-ratio can vary between zero to infinity, and higher values indicate the prominent effect of dams on river flow. We identified sub-basins with a greater influence on dams based on the C-ratio. We find that Beas, Brahmani, upper Satluj, Upper Godavari, Middle and Lower Krishna, and Vashishti are among the most influenced by the dams. Beas sub-basin has the highest C-ratio (4.16) among all the sub-basin in the Indian sub-continent (Figure 7a). Out of the 80 sub-basins, only eleven have C-ratio greater

than 0.5. 64 out of 80 sub-basins have a C-ratio between zero to 0.42 (Figure 7a). We considered only 51 major reservoirs in our analysis. However, there are several major and minor dams for which observed data is unavailable. Therefore, the influence of reservoirs based on the C-ratio might need to be considered. However, our analysis indicates that dams in a few sub-basins can significantly alter the river flow and flood risk. For instance, dams effectively alter extreme flow's timing, duration, and frequency (Mittal et al., 2016). C-ratio alone may not effectively capture the influence of dams on floods; therefore, we multiplied the fractional area affected by floods and the C-ratio for each sub-basins. For instance, if a sub-basin is considerably affected by dams and has a large flood extent, the value of the multiplied ratio will be higher. The multiplier ratio can effectively identify the sub-basins with high flood-affected areas and flow regulated by the reservoirs. We find that Beas, Brahmani, Ravi, and Lower Satluj are among the highly influenced by floods and the presence of reservoirs. Overall, the sub-basins with higher C ratio and the highest flood-affected area are across the Indian subcontinent. Central India has sub-basins that are relatively less affected by floods and the presence of dams.

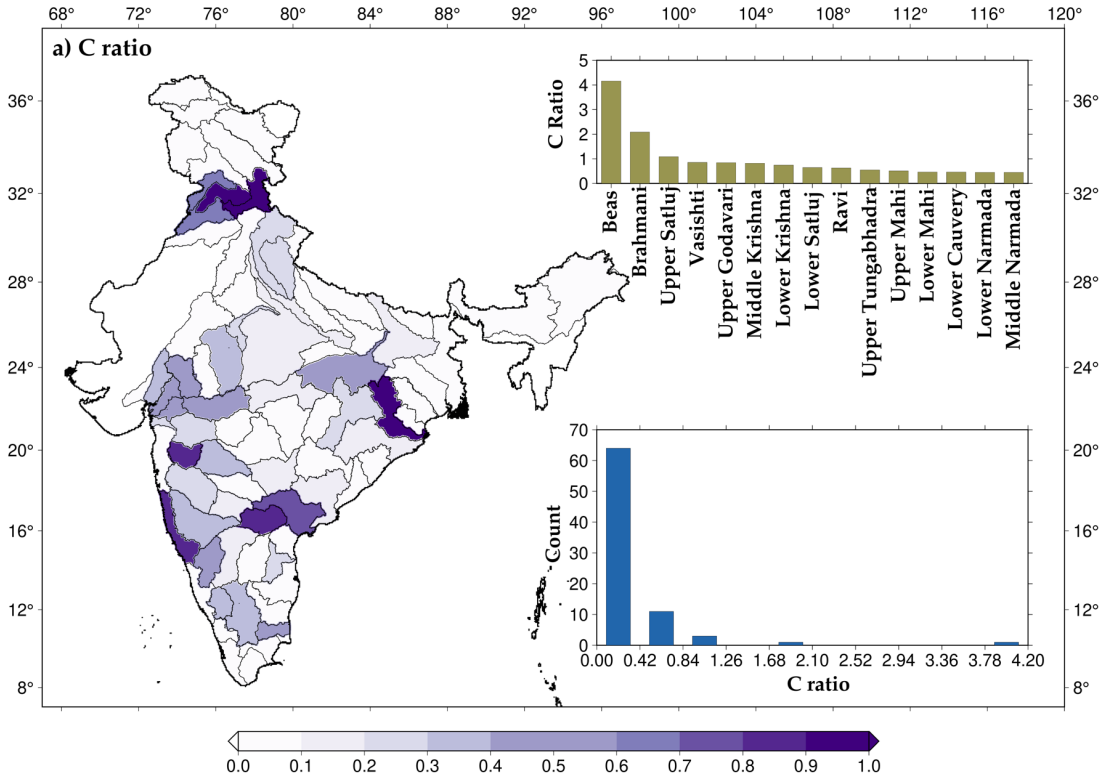
a) C ratio
C Ratio
Beas
Brahmani
Upper Satluj
Vasishti
Upper Godavari
Middle Krishna
Lower Krishna
Lower Satluj
Ravi
Upper Tungabhadra
Upper Mahi
Lower Mahi
Lower Cauvery
Lower Narmada
Middle Narmada
Count
C ratio
0.0 0.1 0.2 0.3 0.4 0.5 0.6 0.7 0.8 0.9 1.0

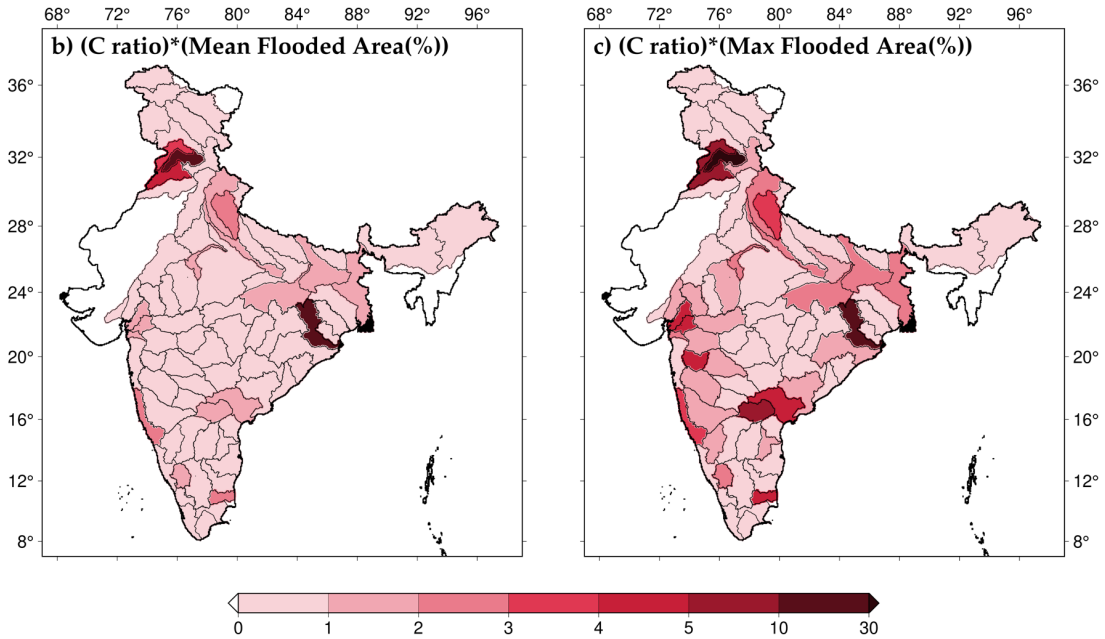
b) (C ratio)*(Mean Flooded Area(%))
c) (C ratio)*(Max Flooded Area(%))
0 1 2 3 4 5 10 30

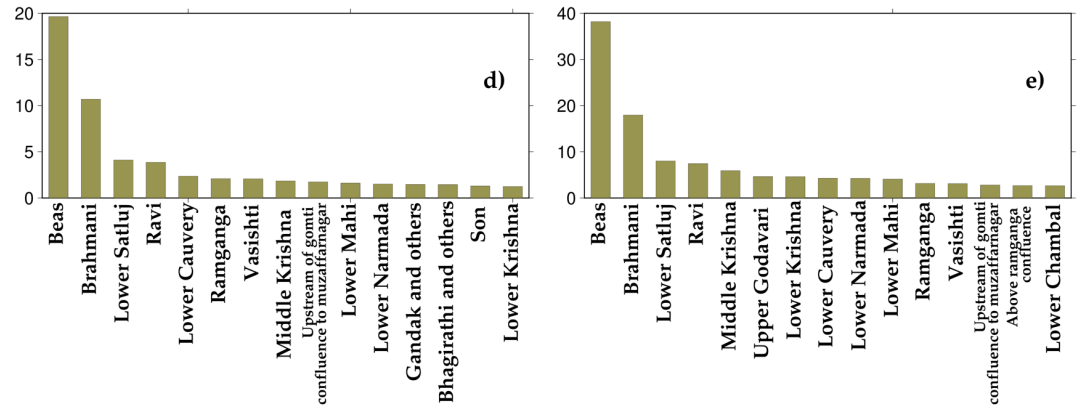
d)
Beas
Brahmani
Lower Satluj
Ravi
Lower Cauvery
Ramganga
Vasishti
Middle Krishna
Upstream of gonti confluence to muzaffarnagar
Lower Mahi
Lower Narmada
Gandak and others
Bhagirathi and others
Son
Lower Krishna
e)
Beas
Brahmani
Lower Satluj
Ravi
Middle Krishna
Upper Godavari
Lower Krishna
Lower Cauvery
Lower Narmada
Lower Mahi
Ramganga
Vasishti
Upstream of gonti confluence to muzaffarnagar
Above ramganga confluence
Lower Chambal

319

Figure 7: (a) Sub-basin wise C-ratio, top fifteen sub-basins and distribution of sub-basins based on C-ratio values (b) Mean of annual maximum flooded area (percentage) multiplied with C-ratio (d) highlighting top 15 sub-basins (c) Historical maximum flooded area (percentage) multiplied with C-ratio (e) highlighting top 15 sub-basins.

3.4 Sub-basin level flood risk assessment

Next, we identified the roads (national highways) and railway exposure to riverine floods for each subbasin. Climate change will adversely affect rail and road networks (Hooper & Chapman, 2012; Padhra, 2022). A considerable length of roads is affected due to surface flooding resulting from high-intensity rain (Koks et al., 2019). Therefore, we examined the impact of floods on rail and road infrastructure in India. We estimated the length of the road and railway network potentially affected by the worst flood that occurred during 1901-2020. We overlapped the road and rail network over the flooded area and estimated the network length exposed to floods (Figures 8a-b). The estimated length for each sub-basin was normalized between zero and one (Figures 8c-d). We find that the road network can be the most affected by the floods in the Gandak, Kosi and Ghaghara confluence to Gomti confluence in the Ganga river basin. On the other hand, a considerable part of the rail network can be affected by floods in Son, Kosi, and Upper Yamuna subbasins. Moreover, in Bhagirathi and Gandak river basins, more than 50 km of road network falls in the flood-prone regions (Figure 8e). There are ten sub-basins in which more than 20 km of road network falls in flood-prone areas of India. Similarly, over 20 km of the rail network is in the flood-affected areas of the six sub-basins (Upper Yamuna, Son, Kosi, Brahmani) [Figure 8f].

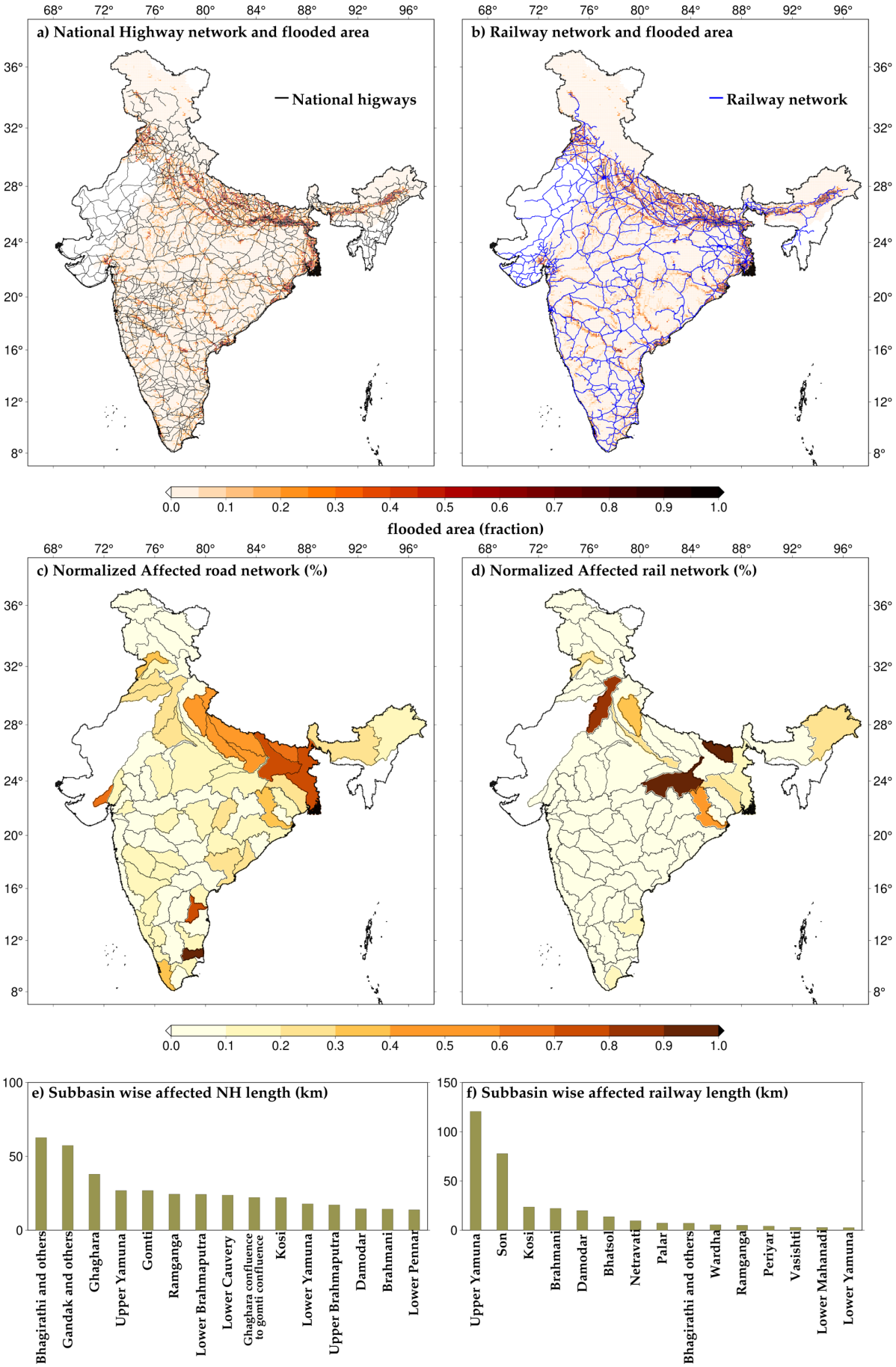
a) National Highway network and flooded area
National higways
b) Railway network and flooded area
Railway network
flooded area (fraction)
c) Normalized Affected road network (%)
d) Normalized Affected rail network (%)
e) Subbasin wise affected NH length (km)
Bhagirathi and others
Gandak and others
Ghaghara
Upper Yamuna
Gomti
Ramganga
Lower Brahmaputra
Lower Cauvery
Ghaghara confluence to gomti confluence
Kosi
Lower Yamuna
Upper Brahmaputra
Damodar
Brahmani
Lower Pennar
f) Subbasin wise affected railway length (km)
Upper Yamuna
Son
Kosi
Brahmani
Damodar
Bhatsol
Netravati
Palar
Bhagirathi and others
Wardha
Ramganga
Periyar
Vasishti
Lower Mahanadi
Lower Yamuna

338

Figure 8: Flood impacts on roads and railways infrastructure. (a-b) National Highways network and Railway network overlapped over the flooded area in worst flood cases, (c-d) subbasin wise normalised flood affected road and railway network (percentage), (e-f) top 15 subbasins with most affected national highways and railway length (km).

Finally, we estimated sub-basin level flood risk using normalized vulnerability, hazard, and exposure (Figure 9). Vulnerability for each sub-basin in India was assessed using the national vulnerability assessment data available at the district level. We estimated hazard probability considering 50% of the inundated area for the worst flood as a benchmark. The likelihood of flood inundated areas in a sub-basin exceeding the benchmark was used in the risk assessment. Similarly, we used the worst flood extent and gridded population data to estimate flood exposure. The sub-basins in north-central India have a relatively higher vulnerability calculated using the socio-economic indicators. The vulnerability is relatively lower in north India and the Western Ghats. Kosi, Gandak, and Damodar sub-basins have the highest vulnerability. We find that hazard probability is higher in the sub-basins of Brahmaputra, rivers in the western Ghats, and a few sub-basins of the Indus river basin (Figure 9b). For instance, upper Satluj, Chenab, and Jhelum sub-basins of the Indus river have higher hazard probability. Other than the Western Ghats, most sub-basins in Peninsular India have relatively lesser hazard probability. Exposure, which represents the fraction of the population affected by flood under the worst flood scenario, is higher in the Indo-Gangetic Plain. Apart from the sub-basins of the Ganga River basin, the lower Brahmaputra, lower Godavari, and Baitarani sub-basin show higher exposure. Therefore, Ganga and Brahmaputra Rivers basins are the highest flood-prone river basins and have high flood exposure. Rentschler et al. (2022) also reported that the highest population exposure due to floods is in Uttar Pradesh, Bihar, and West Bengal, which is part of the Ganga river basin.

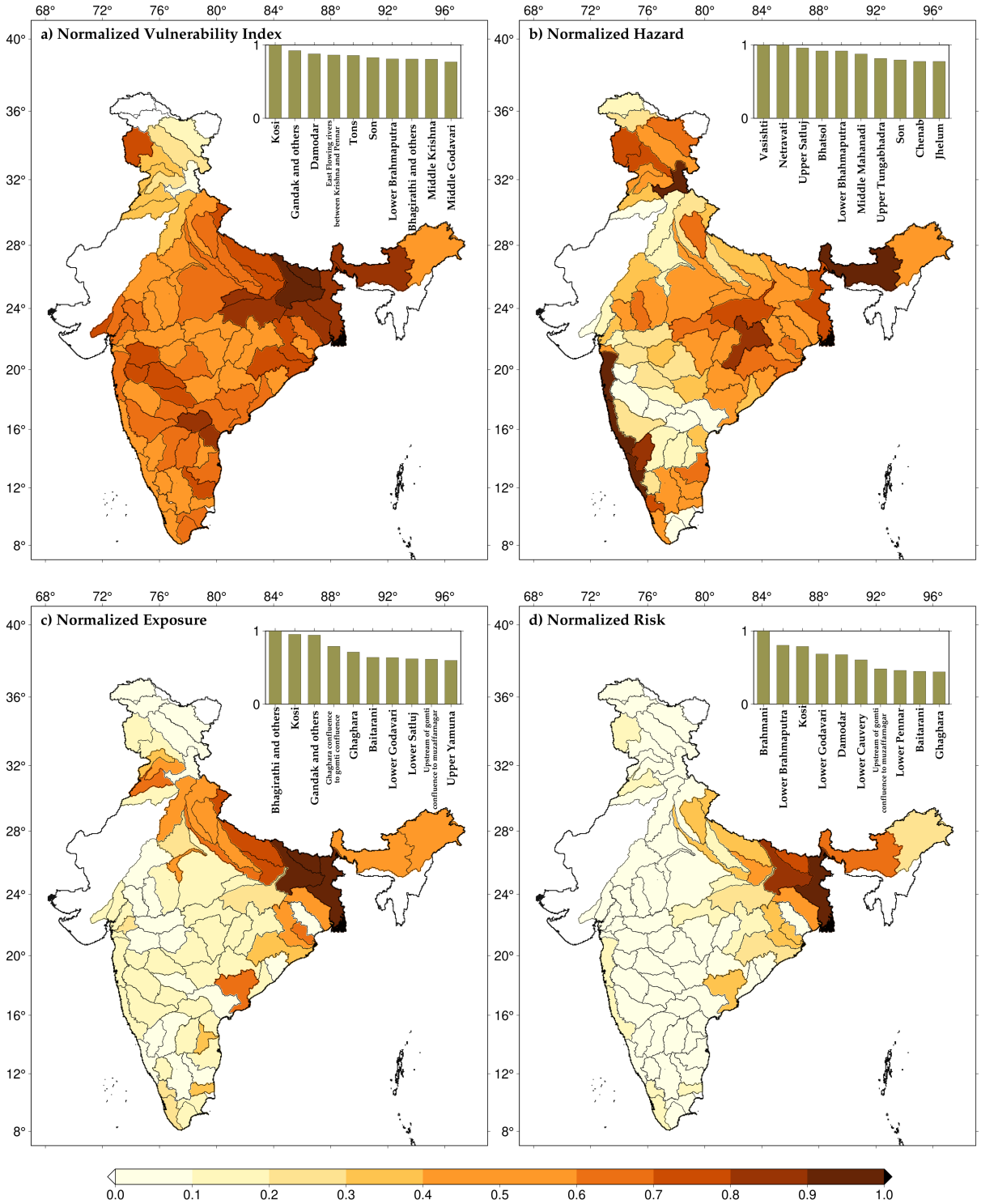

Figure 9: Sub-basin level (a) Normalized vulnerability index (b) Normalized hazard (c) Normalized exposure (d) Normalized risk. The top 10 sub-basins are highlighted as bars in panels inside the figures.

We estimated the flood risk for each sub-basin, a collective representation of vulnerability, hazard, and exposure. As expected, the flood risk is higher in the Ganga and Brahmaputra river basins compared to other parts of the country. The higher flood risk in these basins can be attributed to higher vulnerability, hazard probability, and exposure. For instance, Bhagirathi, Gandak, Kosi, lower Brahmaputra, and Ghaghra are the sub-basins with the highest flood risk in India (Figure 9d). Despite the higher hazard probability in the sub-basins of the Indus and

west coast river basins, the overall flood-risk is considerably lower than the sub-basins of the Ganga and Brahmaputra river basins primarily due to less vulnerability and exposure. Our results show that flood risk in some of the sub-basins of the Ganga and Brahmaputra river basins can be reduced by reducing the vulnerability.

4. Discussion and conclusions

Flood risk mapping is essential for risk reduction and developing mitigation measures. The flood risk will likely increase due to increased hazard probability and exposure (Ali et al., 2019). Hirabayashi et al. (2013) showed that a warmer climate would increase the risk of floods on a global scale. In India also, floods are expected to become more likely under warming climate. For instance, Ali et al. (2019) reported that multi-day floods are projected to rise faster than single-day flood events. The projected rise in the flood frequency in India can be attributed to increased extreme precipitation under warming climate (Mukherjee et al., 2018). Observational studies have also concluded that there has been a considerable rise in extreme precipitation in India during the summer monsoon season (Roxy et al., 2017), which is linked to warming climate. While the warming climate is directly linked to the increased frequency of extreme precipitation, its association with riverine floods is not straightforward. For instance, Nanditha & Mishra (2021, 2022) reported that multi-day precipitation on the wet antecedent condition is the most favourable conditions for riverine floods in India.

While mapping the flood risk at appropriate spatial resolution is complex and challenging, it is vital for disaster risk reduction. Flood inundation mapping that provides the spatial extent of flooding is crucial as the first responders use it during a flood emergency (Apel et al., 2009). There are several approaches to mapping flood inundation (Teng et al., 2017). Various hydrological models have been employed for conducting flood risk assessments at a global scale (Dottori et al., 2018; Gu et al., 2020; Tabari et al., 2021). For instance, Dottori et al. (2018) used the H08 model combined with CaMa-Flood model to estimate losses resulting from river flooding at the country level. Additionally, the LISFLOOD model (van der Knijff et al., 2010) at 5 km spatial resolution was used to estimate the river flood risk in Europe (Alfieri et al., 2018). Flood risk assessment at relatively larger scales are conducted using the coarse resolution land surface hydrological models. The objective of these large scale flood risk assessment is to identify regions that are flood-prone (Dottori et al., 2018; Gu et al., 2020; Tabari et al., 2021). On the other hand, high resolution flood inundation mapping is needed to understand the local flood risk and damage caused to infrastructure. For the analysis of flood inundation during a particular floodat a local scale, high-resolution models such as HEC-RAS and Mike FLOOD can be employed (Khalaj et al., 2021; Nguyen et al., 2016). High resolution flood risk mapping requires comprehensive information of high-resolution topography, cross-sections of channels, and data associated to structural measures of flood protection. However, the smallest subbasin considered in our study has more than 5000 km² area (Fig S7), while most subbasins have area between 10,000 and 50,000 km², with Lower Yamuna being the largest subbasin, with an area of 124,867.19 km². Therefore, the performance of our modelling framework against the satellite and other observations can be considered satisfactory to provide a sub-basin scale flood risk assessment. Moreover, we used hydrodynamic modelling to develop long-term flood inundation maps for the Indian sub-basins. The long-term data (1901-2020) provides us a record of several floods, which can help in robust estimates of flood risk in different sub-basins.

While high-resolution models are suitable for event-specific finer-level flood assessments, their feasibility diminishes in studies involving large-scale flood inundation over longer durations (Yamazaki et al., 2018b). Creating high-resolution flood inundation maps based on hydrodynamic modelling is computationally expensive (Dottori et al., 2016) for a large domain like India. In addition, higher-resolution flood risk mapping that can be used at the local scale for decision-making requires accurate terrain information and river cross-section datasets that are not available. For instance, freely available digital elevation models (DEM) can be too coarse to resolve the flood inundation and depth variability at a local scale (Cook & Merwade, 2009; Dey et al., 2022). The uncertainties within hydrologic outputs can primarily arise due to inaccuracies in both input data and model parameterization (Poulin et al., 2011). Inaccuracies in input meteorological data may stem from disparate sources, leading to errors in spatial and temporal interpolation (Brown & Heuvelink, 2005). Similarly, model parameterization errors, which involve assigning values to parameters governing diverse hydrological processes, can emerge during the calibration process (Laiolo et al., 2015). Moreover, there are uncertainties originating from utilizing long-term flood occurrence data to assess flood mapping capabilities. Our modelling framework that considers the influence of reservoirs provides sub-basin scale flood inundation extent as our aim was to provide a long-term assessment of flood extent in at the country scale. Additionally, downscaling of flood depths introduces biases as coarse-scale information is translated to the local scale (He et al., 2021), which might have considerable deviations from the actual observed flood extent. Given these limitations, our findings provide valuable information based on the long-term record developed using model simulations that can be used for the regional scale policy development for flood mitigation. Cloud cover during the summer monsoon, when most floods occur in India (Nanditha et al., 2022), hinders the utility of satellite data for flood inundation mapping. We calibrated and evaluated our H08-CaMa flood modelling framework using the observed flow, reservoir storage, and satellite-based inundation. However, all these datasets available from the in-situ network or satellites are prone to errors and uncertainty (Di Baldassarre & Montanari, 2009; Stephens et al., 2012; Teng et al., 2017). We used C-ratio as an indicator to quantify the influence of dams on streamflow. However, C-ratio may not fully capture the complexities and variations in the impacts of reservoir operations. Furthermore, in case of run-of-the-river (RoR) dams, the C-ratio may over-estimate the downstream hydrological impacts. Therefore, C-ratio may not solely capture the downstream hydrological effects resulting from dams. Nevertheless, it provides preliminary information on the potential dam influence on the downstream flow.

India has implemented several flood risk mitigation measures at multiple government levels. The construction of embankments along rivers is a common flood risk mitigation measure in India. These embankments help contain the floodwaters within the river channels and protect nearby areas from inundation (NDMA, 2016). The CWC in India operates a network of flood forecasting stations that collect real-time data on rainfall and water levels to forecast floods and issue warnings to vulnerable communities. Notwithstanding the considerable investments and flood-control measures, India has witnessed substantial mortality, human migration, and economic loss. Flood mortality has increased mainly because of increased frequency, not necessarily due to increased flood intensity (Hu et al., 2018). About 3% of the total geographical area of India is affected by floods every year that cause damage to agriculture and infrastructure. The top ten floods that occurred during 1985-2015 caused the mortality of more than 1000 people while more than 35 million people were displaced due to floods between 2000-2004 (Dartmouth Flood Observatory). The recent riverine floods in Uttarakhand and Kerala highlighted the growing flood risk in India, which warrants the need for flood mitigation. The recent flood in August 2022 in Pakistan

caused an estimated loss of $30 billion. Both structural and non-structural measures are required for flood mitigation (Nanditha & Mishra, 2021). Our risk assessment provides policy implications towards reducing vulnerability to reduce the flood risk. Moreover, a sub-basin level ensemble forecast is needed to be used for early flood warnings in the sub-basins with higher flood risk.

Based on our findings, the following conclusions can be made:

- The coupled hydrological and hydrodynamic modelling framework based on the H08-CaMa Flood model was used to estimate the flood risk assessment in India. The hydrological modelling framework performed well against the observed flow, reservoir storage, and satellite-based flood inundation. The role of 51 major reservoirs was considered in flood risk assessment based on the long-term simulations for the 1901-2020 period.
- The sub-basins in the Ganga and Brahmaputra river basins experienced the most significant flood extent during the worst flood in 1901-2020. Similarly, the mean annual maximum flood extent is higher for the sub-basins in the two major transboundary river basins (e.g., Ganga and Brahmaputra). The worst flood affected different sub-basins on the two main flood-affected river basins in different years. Major floods in the flood-prone sub-basins of the Ganga and Brahmaputra basins occur during the summer monsoon season, especially during the August-September period.
- The sub-basins with a more prominent influence of dams based on the C-ratio were identified. Beas, Brahmani, upper Satluj, Upper Godavari, Middle and Lower Krishna, and Vashishti sub-basins are among the most influenced by the dams. Moreover, Beas, Brahmani, Ravi, and Lower Satluj are among the most affected by floods and the presence of reservoirs.
- Flood risk is higher in the Ganga and Brahmaputra river basins compared to other parts of the country. The higher flood risk in the two transboundary river basins can be attributed to higher vulnerability, hazard probability, and exposure. Bhagirathi, Gandak, Kosi, lower Brahmaputra, and Ghaghra are India's sub-basins with the highest flood risk.

Data availability: All the datasets used in this study can be obtained from the corresponding author.

Competing interest: Authors declare no competing interest.

Author contributions: VM designed the study. UV conducted the analysis and wrote the first draft. All the authors contributed in the writing and discussion.

Acknowledgement: The work was supported by the Monsoon Mission, Ministry of Earth Sciences. The authors acknowledge the data availability from India Meteorological Department (IMD) and India-WRIS. We acknowledge the database availability from EM-DAT: http://www.emdat.be/, DFO: http://floodobservatory.colorado.edu, population data from GHSL: https://sedac.ciesin.columbia.edu/data/set/ghsl-population-built-up-estimates-degree-urban-smod, vulnerability assessment data from DST: HYPERLINK "https://dst.gov.in/sites/default/files/Full%20Report%20%281%29.pdf"https://dst.gov.in/sites/default/files/Full%20Report%20%281%29

References

Acreman, M. (2000). *Managed Flood Releases from Reservoirs: Issues and Guidance*. https://sswm.info/sites/default/files/reference_attachments/ACREMAN%202000%20Managed%20Flood%20Releases%20from%20Reservoirs.pdf

Agarwal, A., & Narain, S. (1991). *Floods, flood plains and environmental myths*.

Alfieri, L., Dottori, F., Betts, R., Salamon, P., & Feyen, L. (2018). Multi-Model Projections of River Flood Risk in Europe under Global Warming. *Climate 2018, Vol. 6, Page 6*, *6*(1), 6. https://doi.org/10.3390/CLI6010006

Ali, H., Modi, P., & Mishra, V. (2019). Increased flood risk in Indian sub-continent under the warming climate. *Weather and Climate Extremes*, *25*, 100212. https://doi.org/10.1016/J.WACE.2019.100212

Allen, S. K., Linsbauer, A., Randhawa, S. S., Huggel, C., Rana, P., & Kumari, A. (2016). Glacial lake outburst flood risk in Himachal Pradesh, India: an integrative and anticipatory approach considering current and future threats. *Natural Hazards*, *84*(3), 1741–1763. https://doi.org/10.1007/s11069-016-2511-x

Apel, H., Aronica, G. T., Kreibich, H., & Thieken, A. H. (2009). Flood risk analyses - How detailed do we need to be? *Natural Hazards*, *49*(1), 79–98. https://doi.org/10.1007/S11069-008-9277-8/TABLES/5

Bernhofen, M. V., Cooper, S., Trigg, M., Mdee, A., Carr, A., Bhave, A., Solano-Correa, Y. T., Pencue-Fierro, E. L., Teferi, E., Haile, A. T., Yusop, Z., Alias, N. E., Sa'adi, Z., Bin Ramzan, M. A., Dhanya, C. T., & Shukla, P. (2022). The Role of Global Data Sets for Riverine Flood Risk Management at National Scales. *Water Resources Research*, *58*(4). https://doi.org/10.1029/2021wr031555

Birkmann, J., & Welle, T. (2015). Assessing the risk of loss and damage: Exposure, vulnerability and risk to climate-related hazards for different country classifications.

International Journal of Global Warming, *8*(2), 191–212. https://doi.org/10.1504/IJGW.2015.071963

Boulange, J., Hanasaki, N., Yamazaki, D., & Pokhrel, Y. (2021). Role of dams in reducing global flood exposure under climate change. *Nature Communications*, *12*(1). https://doi.org/10.1038/s41467-020-20704-0

Brown, J. D., & Heuvelink, G. B. M. (2005). Assessing Uncertainty Propagation through Physically Based Models of Soil Water Flow and Solute Transport. *Encyclopedia of Hydrological Sciences*. https://doi.org/10.1002/0470848944.HSA081

Chaudhari, S., & Pokhrel, Y. (2022). Alteration of River Flow and Flood Dynamics by Existing and Planned Hydropower Dams in the Amazon River Basin. *Water Resources Research*, *58*(5). https://doi.org/10.1029/2021WR030555

Chuphal, D. S., & Mishra, V. (2023). Hydrological model-based streamflow reconstruction for Indian sub-continental river basins, 1951–2021. *Scientific Data 2023 10:1*, *10*(1), 1–11. https://doi.org/10.1038/s41597-023-02618-w

Cook, A., & Merwade, V. (2009). Effect of topographic data, geometric configuration and modeling approach on flood inundation mapping. *Journal of Hydrology*, *377*(1–2), 131–142. https://doi.org/10.1016/J.JHYDROL.2009.08.015

Dang, H., Pokhrel, Y., Shin, S., Stelly, J., Ahlquist, D., & Du Bui, D. (2022). Hydrologic balance and inundation dynamics of Southeast Asia's largest inland lake altered by hydropower dams in the Mekong River basin. *Science of The Total Environment*, *831*, 154833. https://doi.org/10.1016/J.SCITOTENV.2022.154833

Dang, T. D., Chowdhury, A. K., & Galelli, S. (2019). On the representation of water reservoir storage and operations in large-scale hydrological models: implications on model parameterization and climate change impact assessments. *Hydrology and Earth System Sciences Discussions*, 1–34. https://doi.org/10.5194/hess-2019-334

Dangar, S., & Mishra, V. (2021). Natural and anthropogenic drivers of the lost groundwater from the Ganga River basin. *Environmental Research Letters*, *16*(11). https://doi.org/10.1088/1748-9326/ac2ceb

de Moel, H., Jongman, B., Kreibich, H., Merz, B., Penning-Rowsell, E., & Ward, P. J. (2015). Flood risk assessments at different spatial scales. *Mitigation and Adaptation Strategies for Global Change*, *20*(6), 865–890. https://doi.org/10.1007/s11027-015-9654-z

Dey, S., Saksena, S., Winter, D., Merwade, V., & McMillan, S. (2022). Incorporating Network Scale River Bathymetry to Improve Characterization of Fluvial Processes in Flood Modeling. *Water Resources Research*, *58*(11), e2020WR029521. https://doi.org/10.1029/2020WR029521

Di Baldassarre, G., & Montanari, A. (2009). Uncertainty in river discharge observations: A quantitative analysis. *Hydrology and Earth System Sciences*, *13*(6), 913–921. https://doi.org/10.5194/HESS-13-913-2009

Dottori, F., Salamon, P., Bianchi, A., Alfieri, L., Hirpa, F. A., & Feyen, L. (2016). Development and evaluation of a framework for global flood hazard mapping. *Advances in Water Resources*, *94*, 87–102. https://doi.org/10.1016/J.ADVWATRES.2016.05.002

Dottori, F., Szewczyk, W., Ciscar, J. C., Zhao, F., Alfieri, L., Hirabayashi, Y., Bianchi, A., Mongelli, I., Frieler, K., Betts, R. A., & Feyen, L. (2018). Increased human and economic losses from river flooding with anthropogenic warming. *Nature Climate Change 2018 8:9*, *8*(9), 781–786. https://doi.org/10.1038/s41558-018-0257-z

Duc Dang, T., Kamal Chowdhury, A. F. M., & Galelli, S. (2020). On the representation of water reservoir storage and operations in large-scale hydrological models: Implications on model parameterization and climate change impact assessments. *Hydrology and Earth System Sciences*, *24*(1), 397–416. https://doi.org/10.5194/HESS-24-397-2020

Eidsvig, U. M. K., Kristensen, K., & Vangelsten, B. V. (2017). Assessing the risk posed by natural hazards to infrastructures. *Natural Hazards and Earth System Sciences*, *17*(3), 481–504. https://doi.org/10.5194/nhess-17-481-2017

Fredrick, O. (2017, May 19). Excavators allege debris was used to bury storey in Chhatar Manzil. *Hindustan Times*. https://www.hindustantimes.com/lucknow/excavators-allege-debris-was-used-to-bury-storey-in-chhatar-manzil/story-mMm8Dwog3azR6SSEmpvjIO.html

Gaur, A., & Gaur, A. (2018). *Future Changes in Flood Hazards across Canada under a Changing Climate*. https://doi.org/10.3390/w10101441

Ghosh, A., & Kar, S. K. (2018). Application of analytical hierarchy process (AHP) for flood risk assessment: a case study in Malda district of West Bengal, India. *Natural Hazards*, *94*(1), 349–368. https://doi.org/10.1007/s11069-018-3392-y

Gu, X., Zhang, Q., Li, J., Chen, D., Singh, V. P., Zhang, Y., Liu, J., Shen, Z., & Yu, H. (2020). *Impacts of anthropogenic warming and uneven regional socio-economic development on global river flood risk*. https://doi.org/10.1016/j.jhydrol.2020.125262

Hanasaki, N., Kanae, S., Oki, T., Masuda, K., Motoya, K., Shirakawa, N., Shen, Y., & Tanaka, K. (2008). An integrated model for the assessment of global water resources - Part 1: Model description and input meteorological forcing. *Hydrology and Earth System Sciences*, *12*(4), 1007–1025. https://doi.org/10.5194/HESS-12-1007-2008

Hanasaki, N., Yoshikawa, S., Pokhrel, Y., & Kanae, S. (2018). A global hydrological simulation to specify the sources of water used by humans. *Hydrology and Earth System Sciences*, *22*(1), 789–817. https://doi.org/10.5194/hess-22-789-2018

He, X., Bryant, B. P., Moran, T., Mach, K. J., Wei, Z., & Freyberg, D. L. (2021). Climate-informed hydrologic modeling and policy typology to guide managed aquifer recharge. *Science Advances*, *7*(17), 6025–6046. https://doi.org/10.1126/SCIADV.ABE6025/SUPPL_FILE/ABE6025_SM.PDF

Hirabayashi, Y., Mahendran, R., Koirala, S., Konoshima, L., Yamazaki, D., Watanabe, S., Kim, H., & Kanae, S. (2013). Global flood risk under climate change. *Nature Climate Change*, *3*(9), 816–821. https://doi.org/10.1038/nclimate1911

583 Hirabayashi, Y., Tanoue, M., Sasaki, O., Zhou, X., & Yamazaki, D. (2021). Global exposure to
584 flooding from the new CMIP6 climate model projections. *Scientific Reports*, *0123456789*,
585 1–7. https://doi.org/10.1038/s41598-021-83279-w

586 Hochrainer-Stigler, S., Schinko, T., Hof, A., & Ward, P. J. (2021). Adaptive risk management
587 strategies for governments under future climate and socioeconomic change: An application
588 to riverine flood risk at the global level. *Environmental Science and Policy*, *125*, 10–20.
589 https://doi.org/10.1016/j.envsci.2021.08.010

590 Hooper, E., & Chapman, L. (2012). The impacts of climate change on national road and rail
591 networks. In *Transport and Sustainability* (Vol. 2, pp. 105–136). Emerald Group
592 Publishing Ltd. https://doi.org/10.1108/S2044-9941(2012)0000002008

593 Hu, P., Zhang, Q., Shi, P., Chen, B., & Fang, J. (2018). Flood-induced mortality across the
594 globe: Spatiotemporal pattern and influencing factors. *Science of The Total Environment*,
595 *643*, 171–182. https://doi.org/10.1016/J.SCITOTENV.2018.06.197

596 IPCC. (2014). *Climate Change 2014: Synthesis Report. Contribution of Working Groups I, II,*
597 *and III to the Fifth Assessment Report of the. Geneva, Switzerland: Intergovernmental*
598 *Panel on Climate Change.*

599 Jain, G., Singh, C., Coelho, K., & Malladi, T. (2017). *Long-term implications of humanitarian*
600 *responses The case of Chennai*.
601 http://pubs.iied.org/10840IIEDwww.iied.org@iiedwww.facebook.com/theIIED

602 Joint Research Centre (JRC), European Commission and Center for International Earth Science
603 Information Network (CIESIN), & Columbia University. (2021). *Global Human Settlement*
604 *Layer: Population and Built-Up Estimates, and Degree of Urbanization Settlement Model*
605 *Grid. Palisades, NY: NASA Socioeconomic Data and Applications Center (SEDAC)*.
606 https://doi.org/10.7927/h4154f0w

607 Joshi, V. (2014, September 14). Have we learnt from past floods? Clearly not! *Hindustan Times*
608 *(Lucknow)*. https://www.pressreader.com/india/hindustan-times-
609 lucknow/20140914/281646778342401

610 Kalantari, Z., Briel, A., Lyon, S. W., Olofsson, B., & Folkeson, L. (2014). On the utilization of
611 hydrological modelling for road drainage design under climate and land use change.
612 *Science of the Total Environment*, *475*, 97–103.
613 https://doi.org/10.1016/J.SCITOTENV.2013.12.114

614 Khalaj, M. R., Noor, H., & Dastranj, A. (2021). Investigation and simulation of flood inundation
615 hazard in urban areas in Iran. *Geoenvironmental Disasters*, *8*(1), 1–13.
616 https://doi.org/10.1186/S40677-021-00191-1/FIGURES/11

617 Kimuli, J. B., Di, B., Zhang, R., Wu, S., Li, J., & Yin, W. (2021). A multisource trend analysis
618 of floods in Asia-Pacific 1990–2018: Implications for climate change in sustainable
619 development goals. In *International Journal of Disaster Risk Reduction* (Vol. 59). Elsevier
620 Ltd. https://doi.org/10.1016/j.ijdrr.2021.102237

621 Koks, E. E., Rozenberg, J., Zorn, C., Tariverdi, M., Vousdoukas, M., Fraser, S. A., Hall, J. W.,
622 & Hallegatte, S. (2019). A global multi-hazard risk analysis of road and railway

infrastructure assets. *Nature Communications*, *10*(1). https://doi.org/10.1038/s41467-019-10442-3

Krysanova, V., Donnelly, C., Gelfan, A., Gerten, D., Arheimer, B., Hattermann, F., & Kundzewicz, Z. W. (2018). How the performance of hydrological models relates to credibility of projections under climate change. *Hydrological Sciences Journal*, *63*(5), 696–720. https://doi.org/10.1080/02626667.2018.1446214

Kushwaha, A. P., Tiwari, A. D., Dangar, S., Shah, H., Mahto, S. S., & Mishra, V. (2021). Multimodel assessment of water budget in Indian sub-continental river basins. *Journal of Hydrology*, *603*, 126977. https://doi.org/10.1016/J.JHYDROL.2021.126977

Laiolo, P., Gabellani, S., Campo, L., Cenci, L., Silvestro, F., Delogu, F., Boni, G., Rudari, R., Puca, S., & Pisani, A. R. (2015). Assimilation of remote sensing observations into a continuous distributed hydrological model: Impacts on the hydrologic cycle. *International Geoscience and Remote Sensing Symposium (IGARSS)*, *2015-November*, 1308–1311. https://doi.org/10.1109/IGARSS.2015.7326015

Lehner, B., Liermann, C. R., Revenga, C., Vörömsmarty, C., Fekete, B., Crouzet, P., Döll, P., Endejan, M., Frenken, K., Magome, J., Nilsson, C., Robertson, J. C., Rödel, R., Sindorf, N., & Wisser, D. (2011). High-resolution mapping of the world's reservoirs and dams for sustainable river-flow management. In *Frontiers in Ecology and the Environment* (Vol. 9, Issue 9, pp. 494–502). https://doi.org/10.1890/100125

Marchand, M., Dahm, R., Buurman, J., Sethurathinam, S., & Sprengers, C. (2022). Flood protection by embankments in the Brahmani–Baitarani river basin, India: a risk-based approach. *International Journal of Water Resources Development*, *38*(2), 242–261. https://doi.org/10.1080/07900627.2021.1899899

Mateo, C. M., Hanasaki, N., Komori, D., & Tanaka, K. (2014). Assessing the impacts of reservoir operation to floodplain inundation by combining hydrological, reservoir management, and hydrodynamic models. *AGU Publications*, 7245–7266. https://doi.org/10.1002/2013WR014845.Received

Mateo, C. M. R., Hanasaki, N., Komori, D., Yoshimura, K., Kiguchi, M., Champathong, A., Yamazaki, D., Sukhapunnaphan, T., & Oki, T. (2013). A simulation study on modifying reservoir operation rules: Tradeoffs between flood mitigation and water supply. *IAHS-AISH Proceedings and Reports*, *362*(July), 33–40.

Mateo, C. M. R., Hanasaki, N., Komori, D., Yoshimura, K., Kiguchi, M., Champathong, A., Yamazaki, D., Sukhapunnaphan, T., & Oki, T. (2014). Flood risk and climate change: global and regional perspectives. *Hydrological Sciences Journal*, *59*(1), 1–28. https://doi.org/10.1080/02626667.2013.857411

Mishra, D. K. (2015, March 10). 1948 Floods in Bihar-2 Inaugural flood after Independence – Official Version of Floods and its Aftermath. *SANDRP*. https://sandrp.in/2015/03/10/1948-floods-in-bihar-2-inaugural-flood-after-independence-official-version-of-floods-and-its-aftermath/

Mishra, V., & Shah, H. L. (2018). Hydroclimatological Perspective of the Kerala Flood of 2018. *Journal of the Geological Society of India*, *92*(5), 645–650. https://doi.org/10.1007/s12594-018-1079-3

Mishra, V., Tiwari, A. D., & Kumar, R. (2022). Warming climate and ENSO variability enhance the risk of sequential extremes in India. *One Earth*, *5*(11), 1250–1259. https://doi.org/10.1016/J.ONEEAR.2022.10.013

Mittal, N., Bhave, A. G., Mishra, A., & Singh, R. (2016). Impact of human intervention and climate change on natural flow regime. *Water Resources Management*, *30*(2), 685–699. https://doi.org/10.1007/s11269-015-1185-6

Mohanty, M. P., Mudgil, S., & Karmakar, S. (2020). Flood management in India: A focussed review on the current status and future challenges. In *International Journal of Disaster Risk Reduction* (Vol. 49). Elsevier Ltd. https://doi.org/10.1016/j.ijdrr.2020.101660

Mohapatra, P. K., & Singh, R. D. (2003). Flood management in India. *Natural Hazards*, *28*, 131–143. https://doi.org/10.1177/0019556120120109

Mukherjee, S., Aadhar, S., Stone, D., & Mishra, V. (2018). Increase in extreme precipitation events under anthropogenic warming in India. *Weather and Climate Extremes*, *20*, 45–53. https://doi.org/10.1016/J.WACE.2018.03.005

Nanditha, J. S., Kushwaha, A. P., Singh, R., Malik, I., Solanki, H., Singh Chupal, D., Dangar, S., Shwarup Mahto, S., Mishra, V., Vegad, U., Chuphal, D. S., & Mahto, S. S. (2022). The Pakistan flood of August 2022: causes and implications. *Authorea Preprints*. https://doi.org/10.1002/ESSOAR.10512560.1

Nanditha, J. S., & Mishra, V. (2021). On the need of ensemble flood forecast in India. *Water Security*, *12*, 100086. https://doi.org/10.1016/J.WASEC.2021.100086

Nanditha, J. S., & Mishra, V. (2022). Multiday Precipitation Is a Prominent Driver of Floods in Indian River Basins. *Water Resources Research*, *58*(7), e2022WR032723. https://doi.org/10.1029/2022WR032723

Nguyen, P., Thorstensen, A., Sorooshian, S., Hsu, K., AghaKouchak, A., Sanders, B., Koren, V., Cui, Z., & Smith, M. (2016). A high resolution coupled hydrologic–hydraulic model (HiResFlood-UCI) for flash flood modeling. *Journal of Hydrology*, *541*, 401–420. https://doi.org/10.1016/J.JHYDROL.2015.10.047

Nilsson, C., Catherine, *, Reidy, A., Dynesius, M., & Revenga, C. (2005). Fragmentation and Flow Regulation of the World's Large River Systems. In *SCIENCE* (Vol. 308). www.sciencemag.org

Padhra, A. (2022). Tourism in India and the Impact of Weather and Climate. In *Indian Tourism* (pp. 187–197). Emerald Publishing Limited. https://doi.org/10.1108/978-1-80262-937-820221013

Pai, D. S., Sridhar, L., Rajeevan, M., Sreejith, O. P., Satbhai, N. S., & Mukhopadhyay, B. (2014). Development of a new high spatial resolution (0.25° × 0.25°) long period (1901-

2010) daily gridded rainfall data set over India and its comparison with existing data sets over the region. *Mausam*, *65*(1), 1–18.

Pathak, S., Liu, M., Jato-Espino, D., & Zevenbergen, C. (2020). Social, economic and environmental assessment of urban sub-catchment flood risks using a multi-criteria approach: A case study in Mumbai City, India. *Journal of Hydrology*, *591*, 125216. https://doi.org/10.1016/J.JHYDROL.2020.125216

Peduzzi, P., Dao, H., Herold, C., & Mouton, F. (2009). Natural Hazards and Earth System Sciences Assessing global exposure and vulnerability towards natural hazards: the Disaster Risk Index. In *Hazards Earth Syst. Sci* (Vol. 9). www.nat-hazards-earth-syst-sci.net/9/1149/2009/

Pekel, J. F., Cottam, A., Gorelick, N., & Belward, A. S. (2016). High-resolution mapping of global surface water and its long-term changes. *Nature*, *540*(7633), 418–422. https://doi.org/10.1038/nature20584

Pokhrel, Y., Shin, S., Lin, Z., Yamazaki, D., & Qi, J. (2018). Potential Disruption of Flood Dynamics in the Lower Mekong River Basin Due to Upstream Flow Regulation. *Scientific Reports*, *8*(1). https://doi.org/10.1038/s41598-018-35823-4

Poulin, A., Brissette, F., Leconte, R., Arsenault, R., & Malo, J. S. (2011). Uncertainty of hydrological modelling in climate change impact studies in a Canadian, snow-dominated river basin. *Journal of Hydrology*, *409*(3–4), 626–636. https://doi.org/10.1016/J.JHYDROL.2011.08.057

Raghav, P., & Eldho, T. I. (2023). Investigations on the hydrological impacts of climate change on a river basin using macroscale model H08. *Journal of Earth System Science*, *132*(2), 1–23. https://doi.org/10.1007/S12040-023-02102-4/FIGURES/10

Rentschler, J., Salhab, M., & Jafino, B. A. (2022). Flood exposure and poverty in 188 countries. *Nature Communications*, *13*(1). https://doi.org/10.1038/s41467-022-30727-4

Roxy, M. K., Ghosh, S., Pathak, A., Athulya, R., Mujumdar, M., Murtugudde, R., Terray, P., & Rajeevan, M. (2017). A threefold rise in widespread extreme rain events over central India. *Nature Communications*, *8*(1). https://doi.org/10.1038/s41467-017-00744-9

Roy, B., Khan, M. S. M., Saiful Islam, A. K. M., Khan, M. J. U., & Mohammed, K. (2021). Integrated flood risk assessment of the arial khan river under changing climate using ipcc ar5 risk framework. *Journal of Water and Climate Change*, *12*(7), 3421–3447. https://doi.org/10.2166/wcc.2021.341

Shah, H. L., & Mishra, V. (2016). Hydrologic Changes in Indian Subcontinental River Basins (1901–2012). *Journal of Hydrometeorology*, *17*(10), 2667–2687. https://doi.org/10.1175/JHM-D-15-0231.1

Sheffield, J., Goteti, G., & Wood, E. F. (2006). *Development of a 50-Year High-Resolution Global Dataset of Meteorological Forcings for Land Surface Modeling*.

Singh, A., Mani, M., & Vishnoi, R. K. (2021). Tehri Dam–A Savior from Climate Change Led Extreme Events. *INCOLD Journal (A Half Yearly Technical Journal of Indian Committee on Large Dams)*, *10*(2), 44–50.

Singh, P., Sinha, V. S. P., Vijhani, A., & Pahuja, N. (2018). Vulnerability assessment of urban road network from urban flood. *International Journal of Disaster Risk Reduction*, *28*, 237–250. https://doi.org/10.1016/J.IJDRR.2018.03.017

Smith, A., Bates, P. D., Wing, O., Sampson, C., Quinn, N., & Neal, J. (2019). New estimates of flood exposure in developing countries using high-resolution population data. *Nature Communications*, *10*(1). https://doi.org/10.1038/s41467-019-09282-y

Srivastava, A. K., Rajeevan, M., & Kshirsagar, S. R. (2009). Development of a high resolution daily gridded temperature data set (1969 – 2005) for the Indian region. *Atmospheric Science Letters*, *10*(October), 249–254. https://doi.org/10.1002/asl

Stephens, E. M., Bates, P. D., Freer, J. E., & Mason, D. C. (2012). The impact of uncertainty in satellite data on the assessment of flood inundation models. *Journal of Hydrology*, *414–415*, 162–173. https://doi.org/10.1016/J.JHYDROL.2011.10.040

Tabari, H., Hosseinzadehtalaei, P., Thiery, W., & Willems, P. (2021). Amplified Drought and Flood Risk Under Future Socioeconomic and Climatic Change. *Earth's Future*, *9*(10), e2021EF002295. https://doi.org/10.1029/2021EF002295

Tanoue, M. (2020). *Future river-flood damage increases under aggressive adaptations*. 1–12.

Teng, J., Jakeman, A. J., Vaze, J., Croke, B. F. W., Dutta, D., & Kim, S. (2017). Flood inundation modelling: A review of methods, recent advances and uncertainty analysis. *Environmental Modelling & Software*, *90*, 201–216. https://doi.org/10.1016/J.ENVSOFT.2017.01.006

UNISDR. (2011). *Global Assessment Report on Disaster Risk Reduction 2011, Revealing Risk, Redefining Development, United Nations International Strategy for Disaster Reduction Secretariat, Geneva, 2011*. https://www.undp.org/publications/2011-global-assessment-report-disaster-risk-reduction?utm_source=EN&utm_medium=GSR&utm_content=US_UNDP_PaidSearch_Brand_English&utm_campaign=CENTRAL&c_src=CENTRAL&c_src2=GSR&gclid=CjwKCAiAqaWdBhAvEiwAGAQlttbTEIs1543d8ZuHyzCatyJutiZP2w2Wp41vZBSiouchJ7PvGpIcUBoCxOYQAvD_BwE

UNISDR. (2013). *Global Assessment Report on Disaster Risk Reduction 2013, From Shared Risk to Shared Value: the Business Case for Disaster Risk Reduction, United Nations International Strategy for Disaster Reduction Secretariat, Geneva, 2013*. https://www.undrr.org/publication/global-assessment-report-disaster-risk-reduction-2013

van der Knijff, J. M., Younis, J., & de Roo, A. P. J. (2010). LISFLOOD: a GIS-based distributed model for river basin scale water balance and flood simulation. *International Journal of Geographical Information Science*, *24*(2), 189–212. https://doi.org/10.1080/13658810802549154

776 Varis, O., Taka, M., & Tortajada, C. (2022). Global human exposure to urban riverine floods
777 and storms. *River*. https://doi.org/10.1002/rvr2.1

778 Vu, D. T., Dang, T. D., Galelli, S., & Hossain, F. (2022). Satellite observations reveal 13 years
779 of reservoir filling strategies, operating rules, and hydrological alterations in the Upper
780 Mekong River basin. *Hydrology and Earth System Sciences*, *26*(9), 2345–2364.
781 https://doi.org/10.5194/hess-26-2345-2022

782 Ward, P. J., Jongman, B., Weiland, F. S., Bouwman, A., Van Beek, R., Bierkens, M. F. P.,
783 Ligtvoet, W., & Winsemius, H. C. (2013). Assessing flood risk at the global scale: Model
784 setup, results, and sensitivity. *Environmental Research Letters*, *8*(4).
785 https://doi.org/10.1088/1748-9326/8/4/044019

786 Winsemius, H. C., Jongman, B., Veldkamp, T. I. E., Hallegatte, S., Bangalore, M., & Ward, P. J.
787 (2018). Disaster risk, climate change, and poverty: Assessing the global exposure of poor
788 people to floods and droughts. *Environment and Development Economics*, *23*(3), 328–348.
789 https://doi.org/10.1017/S1355770X17000444

790 Winsemius, H. C., van Beek, L. P. H., Jongman, B., Ward, P. J., & Bouwman, A. (2013). A
791 framework for global river flood risk assessments. *Hydrology and Earth System Sciences*,
792 *17*(5), 1871–1892. https://doi.org/10.5194/hess-17-1871-2013

793 Yamazaki, D., De Almeida, G. A. M., & Bates, P. D. (2013). Improving computational
794 efficiency in global river models by implementing the local inertial flow equation and a
795 vector-based river network map. *Water Resources Research*, *49*(11), 7221–7235.
796 https://doi.org/10.1002/wrcr.20552

797 Yamazaki, D., Kanae, S., Kim, H., & Oki, T. (2011). *A physically based description of*
798 *floodplain inundation dynamics in a global river routing model*. *47*(February), 1–21.
799 https://doi.org/10.1029/2010WR009726

800 Yamazaki, D., Watanabe, S., & Hirabayashi, Y. (2018a). Global Flood Risk Modeling and
801 Projections of Climate Change Impacts. *Global Flood Hazard: Applications in Modeling,*
802 *Mapping, and Forecasting*, *233*, 185–203. http://cmip-pcmdi.llnl.gov/

803 Yamazaki, D., Watanabe, S., & Hirabayashi, Y. (2018b). Global Flood Risk Modeling and
804 Projections of Climate Change Impacts. *Geophysical Monograph Series*, *233*, 185–203.
805 https://doi.org/10.1002/9781119217886.CH11

806 Yang, T., Sun, F., Gentine, P., Liu, W., Wang, H., Yin, J., Du, M., & Liu, C. (2019). Evaluation
807 and machine learning improvement of global hydrological model-based flood simulations.
808 *Environmental Research Letters*, *14*(11). https://doi.org/10.1088/1748-9326/ab4d5e

809 Yoshida, T., Hanasaki, N., Nishina, K., Boulange, J., Okada, M., & Troch, P. A. (2022).
810 Inference of Parameters for a Global Hydrological Model: Identifiability and Predictive
811 Uncertainties of Climate-Based Parameters. *Water Resources Research*, *58*(2),
812 e2021WR030660. https://doi.org/10.1029/2021WR030660

813 Zajac, Z., Revilla-Romero, B., Salamon, P., Burek, P., Hirpa, F., & Beck, H. (2017). The impact
814 of lake and reservoir parameterization on global streamflow simulation. *Journal of*
815 *Hydrology*, *548*, 552–568. https://doi.org/10.1016/j.jhydrol.2017.03.022

816 Zhao, F., Veldkamp, T. I. E., Frieler, K., Schewe, J., Ostberg, S., Willner, S., Schauberger, B.,
817 Gosling, S. N., Schmied, H. M., Portmann, F. T., Leng, G., Huang, M., Liu, X., Tang, Q.,
818 Hanasaki, N., Biemans, H., Gerten, D., Satoh, Y., Pokhrel, Y., … Yamazaki, D. (2017).
819 The critical role of the routing scheme in simulating peak river discharge in global
820 hydrological models. *Environmental Research Letters*, *12*(7). https://doi.org/10.1088/1748-
821 9326/aa7250

822